Accelerated fronts in a two stage invasion process

Matt Holzer and Arnd Scheel
University of Minnesota
School of Mathematics
127 Vincent Hall, 206 Church St SE
Minneapolis, MN 55455, USA

June 11, 2013

Abstract

We study wavespeed selection in a staged invasion process. We consider a model in which an unstable homogeneous state is replaced via an invading front with a secondary state. This secondary state is also unstable and, in turn, replaced by a stable homogeneous state via a secondary invasion front. We are interested in the selected wavespeed of the secondary front. In particular, we investigate conditions under which the influence of the primary front increases this speed. We find three regimes: a locked regime where both fronts travel at the same speed, a pulled regime where the secondary front travels at the linear spreading speed associated to the intermediate state, and an accelerated regime where the selected speed is between these two speeds. We show that the transition to locked fronts can be described by the crossing of a resonance pole in the linearization about the primary front. In addition, using properties of this resonance pole we derive the selected wavespeed in the accelerated case and determine when the transition between accelerated and pulled fronts occurs.

MSC numbers: 35C07, 35K57, 34A26
Keywords: invasion fronts, wavespeed selection, coupled reaction-diffusion equations

1 Introduction

In this paper, we determine the selected wavespeed for the following two component reaction-diffusion system,

$$\begin{aligned} u_t &= u_{xx} + u(1-u) \\ v_t &= dv_{xx} + g(u)v - v^3, \end{aligned} \tag{1.1}$$

where $d > 0$ and $g(u)$ is some nonlinear function. The equation describing the evolution of u is the famous Fisher-KPP equation [12, 17]. It is well known that small, sufficiently localized initial perturbations of the unstable zero state develop into a pair of counter propagating fronts. The selected wavespeed is the asymptotic speed of these fronts, which for the Fisher-KPP model is two. These fronts are pulled, which is to say that their speed is determined solely by the interplay between the diffusion operator and the linear instability of the $u = 0$ state. The nonlinearity is irrelevant as far as wavespeed selection is concerned. The two equations couple through an inhomogeneous linear term, $g(u)$. We are interested in the selected spreading speed of the v component, again supposing sufficiently steep initial data. In analogy to the u component, we suspect from the outset that the selected wavespeed can be determined by only the interaction of the diffusion and the linear instability of the $v = 0$ steady state. However, in contrast with the KPP front, the linear instability of the zero state in the v equation is inhomogeneous in space and time and therefore determining the appropriate spreading speed presents new challenges.

Before stating our results, we pause to motivate the choice of (1.1) as the focus of study in this paper. The first such motivation is to view system (1.1) as describing a rather general formulation of a scalar wavespeed selection problem in an inhomogeneous medium. That is, if one assumes that the u component has reached its asymptotic form as a traveling front moving with speed two, then the evolution of v describes an invasion

problem in an inhomogeneous medium wherein the inhomogeneity is localized and travels with some fixed speed. Note that the function $g(u)$ can be quite general. We remark that studies of wavespeed selection in inhomogeneous problems represent a large and interesting literature, see for example [6, 24, 13, 2, 18] among many others. To focus our attention, we consider the case where the instantaneous spreading speeds associated to the asymptotic rest states $u = 0$ and $u = 1$ are slower than the KPP front. However, we suppose that for some range of u values the instantaneous spreading speeds exceed two. It is natural to expect that if this inhomogeneity is strong enough, then perturbations of the v component can be transported at the same speed as the KPP front. Determining properties of $g(u)$ that lead to this locking is one of the aims of this paper. We remark that in contrast to many of the studies stated above, this problem and our formulation of it lends itself naturally to an analysis via dynamical systems theory.

A second motivation arises from the problem of determining secondary invasion speeds in a staged invasion process. One can imagine a situation where an unstable homogeneous state is perturbed, giving rise to a traveling invasion front that propagates into the surrounding medium and deposits in its wake a secondary state. This secondary state may itself be unstable and give rise to a secondary invasion front. One question of interest is how to determine the selected speed associated to this secondary invasion front. A natural approach is to neglect the primary invasion front and calculate the speed of invasion associated to the secondary unstable homogeneous state. Of course, this ignores any influence of the primary front on the secondary invasion front. Assuming that the secondary invasion speed is slower this may not seem like such an extreme proposition, since eventually the secondary front will be propagating in a medium that is essentially everywhere quenched into the secondary state. However, this assumption is not always appropriate and we will show that even in this case the influence of the primary front on the speed of the secondary front can actually be quite severe.

A specific example of a staged invasion process similar to (1.1) arises in competition between roll and hexagon patterns in pattern forming systems near the onset of a Turing bifurcation. Restricting to an infinite cylinder, amplitude equations can be derived in this limit that consist of a pair of coupled Ginzburg-Landau equations,

$$\begin{aligned} A_T &= 4A_{XX} + \mu A + \alpha_1 B^2 + \alpha_2 A^3 + 2\alpha_3 A B^2 \\ B_T &= B_{XX} + \left(\mu + \alpha_1 A + \alpha_3 A^2\right) B + (\alpha_2 + \alpha_3) B^3, \end{aligned} \tag{1.2}$$

see for example [5, 19]. The homogeneous system has three non-negative fixed points: the unstable state at the origin, the roll state at $(A, B) = (A_R, 0)$ and the hexagonal state at $(A, B) = (A_H, A_H)$. A small, positive perturbation of the zero state will grow and spread. A linear stability analysis of the zero state shows that the pure roll state spreads faster than the hexagonal state. Therefore, on short time scales one observes the formation of a roll state with a subsequent formation of a hexagonal pattern via secondary invasion front. The aim is then to determine the spreading speed associated to this secondary state. This spreading speed is bounded below by the spreading speed associated with the hexagonal invasion of a pure roll state. However, there is no guarantee that this estimate is sharp.

An important feature of these coupled Ginzburg-Landau equations is that the $B = 0$ subspace is invariant. In fact, the existence of an invariant subspace is an essential ingredient to the observed dynamics. This invariant subspace enforces a skew-product structure in the linearization about the zero state and the roll state. For a general system without this skew-product structure, any linearly selected invasion mode will have an eigenfunction with non-zero entries in all components and the full system will evolve in a manner analogous to scalar equations, see [22]. On the other hand, a skew-product structure in the linearization allows for various components to evolve at different speeds and one can observe modes of invasion qualitatively different than those that arise in scalar problems, [23, 15].

Typical results for model (1.1) are shown in Figure 1, where observed wavespeeds for the v component in (1.1) are plotted as the strength of the inhomogeneity is increased through the variation of a single parameter. We find three regimes. When the inhomogeneity is weak, the v front travels with exactly the linear spreading speed associated to the state in the wake of the u front. When the inhomogeneity is very strong these two fronts lock and move with the Fisher speed of 2. In the interim, the v front propagates with a speed somewhere between these two speeds. We make several immediate observations. In the locked case, the speed never exceeds the speed of the u front, even when linearized inhomogeneous dynamics indicate a faster speed of propagation. Thus, the linear spreading speed for perturbations of inhomogeneous media do not necessarily place a lower bound on the spreading speeds for the full system. Second, we consider the

case where the speed is advanced but does lock. We note that due to the difference in the selected speeds of the two components, the front interfaces will eventually be a very large distance apart. Nonetheless, the primary front exerts an influence on the secondary front through a front interaction that remains constant over an increasing large spatial distance. We refer to fronts traveling with speed two as *locked*, fronts moving with speed $2\sqrt{dg(0)}$ as *pulled* and fronts moving with some intermediate speed as *accelerated*. The primary tasks of this article are to determine the parameter values for which the transition from locked to accelerated fronts occurs, to do the same for the transition from pulled to accelerated and to derive a prediction for the selected speed in the accelerated case.

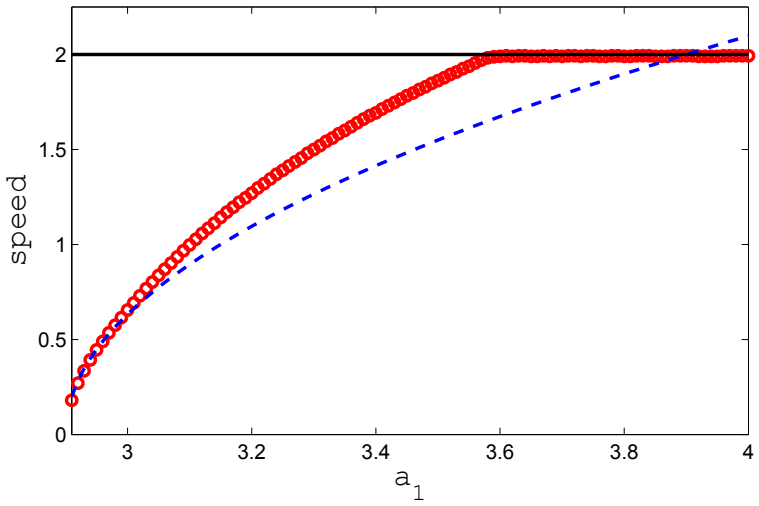

Figure 1: Characteristic behavior of the model (1.1) with $g(u) = a_0 + a_1 u + a_2 u^2$ for $d = 1$, $a_0 = .1$ and $a_2 = -3$. The dashed line is the linear spreading speed of v fronts when $u = 1$ and the solid line is the speed of the KPP front. The circles are numerically derived spreading speeds for the model, showing the speed up of v fronts due to the inhomogeneous coupling.

Finally, we note that this system provides an interesting example of some of the ways in which wavespeed selection mechanisms differ for systems of reaction-diffusion equations as opposed to scalar systems. For scalar equations, invasion fronts are typically classified as pulled or pushed depending on their mode of propagation. Pulled fronts are driven by linear instability of the homogeneous state ahead of the front while pushed fronts are driven by the nonlinearity behind the front. We remark that the fronts in this system of equations sometimes defy this standard classification. Undoubtedly, the u front is a pulled front. However, a characterization of the v front is more elusive. When the inhomogeneity is weak – one example of a weak inhomogeneity is just $g(u)$ constant – then this front is pulled. However, as the strength of this inhomogeneity is increased this situation changes. In some respects the v front behaves like a pushed front in the locked case, although one could argue that it is not really the nonlinearity giving rise to faster invasion speeds but instead the linear behavior of the inhomogeneous medium (a pulled-pulled front). In the accelerated case, the situation is even more murky. Whatever the case may be – and we admit that insisting on such a classification is somewhat pedantic – we see that novel modes of invasion exist for non-scalar equations.

The paper is organized as follows. In section 2, we derive an eigenvalue problem to quantify the strength of the inhomogeneity $g(u)$ and state our main results. In section 3, we demonstrate the existence of locked fronts for sufficiently large strength of the inhomogeneity. Then, in section 4 we investigate the spreading speeds when the inhomogeneity does not induce locking. Finally, in section 5 we conclude with some numerical results that illustrate these behaviors.

2 Characterizing the strength of the inhomogeneity and the main results

Throughout this paper, we will study system (1.1). We make the following assumptions of the inhomogeneous term, $g(u)$,

A1. $g(u) > 0$, i.e. the medium is everywhere unstable for $u \in [0, 1]$,

A2. $\sqrt{dg(1)} < 1$ and $\sqrt{dg(0)} < 1$, i.e. the spreading speeds of the v component at the fixed state ahead of and behind the KPP front are slower than the spreading speed of the KPP front itself.

We are interested in the selected wavespeed for the v equation as $t \to \infty$, supposing that the initial distribution of v is compactly supported. The u equation decouples and is the famous Fisher-KPP equation, [12, 17]. It is well known that compactly supported initial perturbations of the unstable state $u = 0$ develop into a pair of traveling fronts propagating with asymptotic speed two. Our approach is to view the u component as already having approached its asymptotic form of a traveling front solution. We will then determine the selected speed of the v component in this inhomogeneous medium. The first step will be to determine the linear spreading speed of compactly supported perturbations of the unstable state $v = 0$. If this speed exceeds the spreading speed of the KPP front, we will prove the existence of a traveling front for the v equation moving with the same speed as the KPP front.

Let $\xi = x - 2t$ and denote the KPP front $U_{KPP}(\xi)$. We begin with a study of the linearization of (1.1) about the solution $(u, v) = (U_{KPP}, 0)$,

$$q_t = dq_{\xi\xi} + 2q_\xi + g(U_{KPP}(\xi))q. \tag{2.1}$$

The linear response of the v component is then encoded in the spectrum of the operator on the right hand side of (2.1). Of course, since the underlying medium is pointwise unstable so is the spectrum. An important distinction can be made as to whether this instability is absolute or convective. That is to say, localized perturbations undoubtedly grown in norm (say the $L^2(\mathbb{R})$ norm), however they may be convected away from their original location at the same time leading to pointwise decay. Dynamically speaking, if these perturbations grow pointwise then the linearized dynamics in the v component will also spread with speed greater than or equal to two. If instead, the instability is convective and perturbations decay pointwise, then we observe linear propagation speeds of less than two and the KPP front outruns the instability that it generates in the v component.

The aim is then to differentiate between convective and absolute instabilities for the linearized system (2.1). To do this, we follow [20] and consider the spectrum of the linear operator in (2.1) upon restriction to certain exponentially weighted Banach spaces. We use the space,

$$L^2_\sigma(\mathbb{R}) := \{q \in L^2(\mathbb{R}) | q(\xi)e^{\sigma\xi} \in L^2(\mathbb{R})\}. \tag{2.2}$$

In particular, we select $\sigma = d^{-1}$ and let $\tilde{q}(\xi) = q(\xi)e^{\frac{\xi}{d}}$. Then the operator posed on this weighted space is equivalent to the following operator posed on $L^2(\mathbb{R})$,

$$H_g := d\partial_{\xi\xi} + \left(-d^{-1} + g(U(\xi)\right). \tag{2.3}$$

If the spectrum of this operator is stable, then in the un-weighted space perturbations grow but are convected away from their original location. On the other hand, unstable spectrum implies absolute instability and pointwise growth in the moving frame. This provides the basis for our results. If the spectrum of H_g is unstable, then we expect that the v front is locked to the KPP front. Conversely, if the spectrum is stable, then absent nonlinear effects, the selected speed for the v front will be less than that of the KPP front.

To establish locking, we will prove the existence of a traveling front solution to (1.1), moving with speed two. In order for the constructed front to be the selected one, it is required that the front be marginally stable [8]. Marginal stability is the property that compactly supported perturbations of the front neither grow nor decay pointwise in a frame moving with the speed of the front. It is often possible to define marginal stability in terms of spectral properties of the linearized eigenvalue problem about the front posed on an exponentially weighted Banach space. Here the asymptotic decay rates of the front are key, as this

may determine whether the system has a neutrally stable eigenvalue. Steep decay is required so that the expected zero eigenvalue, the derivative of the front profile, remains as an element of the weighted space.

To construct the front, we begin by writing (2.1) as a system of first order equations, $Q' = A(\xi)Q$. This system has three non-negative steady states corresponding to the stable state $(u, v) = (1, \sqrt{g(1)})$, the intermediate state $(1, 0)$ and the unstable state at $(0, 0)$. As is typical of invasion problems, the stable homogeneous state is a saddle point for the traveling front system $Q' = A(\xi)Q$ while the unstable homogeneous state is stable in the traveling front system. We observe the existence of traveling front solutions connecting the unstable and intermediate states (the KPP front) as well as one connecting the intermediate and stable states. This second front satisfies Nagumo's equation and is found by setting $u = 1$ in the equation for v. By our assumptions on the inhomogeneity $g(u)$, the selected speed for the v component with u fixed equal to one is less than two. When viewed in a frame moving with the speed of the faster KPP front, the traveling front connecting the stable and intermediate states is not marginally stable. That is to say that this front approaches the intermediate state along the weaker of the two possible eigendirections; see Figure 2. We will seek traveling front solutions for the full problem that lie close to the concatenation of this Nagumo front and the KPP front. Furthermore, we require that this traveling front solution lies in the strong stable manifold of the unstable state. Since this solution will approach the intermediate state along a weak-stable direction, this will only be possible if the influence of the inhomogeneous term $g(u)$ serves to map this weak stable manifold onto the strong stable manifold during its evolution near the KPP front.

We shall recollect that the location of the leading eigenvalue of the operator H_g is naturally related to exactly this geometric condition. The weighted function space serves to split the spectra of the asymptotic systems $A_\pm = \lim_{\xi\to\pm\infty} A(\xi)$ so that eigenvalues of H_g correspond to solutions of (2.1) whose v component is asymptotic to the weak stable subspace as $\xi \to -\infty$ and asymptotic to the strong stable eigenspace as $\xi \to \infty$. If the leading eigenvalue of H_g is negative, these weak-stable and strong stable subspaces retain their orientation as they evolve from $(1, 0)$ to $(0, 0)$. Alternatively, if this eigenvalue is positive, then these subspaces pass through one another and twist once, or more around, the origin. The nonlinear manifolds tag along for the ride. Using our assumptions on g we will show that that this property leads to traveling front solutions for the full problem that have steep decay in the v component.

We will prove the following result.

Theorem 1. *Assume A1 and A2 above. Suppose that a principle eigenvalue of H_g is positive. Then the selected wavespeed for (1.1) is equal to the selected speed of the u front. That is, there exists a traveling front solution $(U_{KPP}(x - 2t), V(x - 2t))$ where $V(\xi)$ has strong exponential decay with rate $e^{\left(-\frac{1}{d} - \frac{\sqrt{1-dg(0)}}{d}\right)\xi}$ as $\xi \to \infty$.*

When the principle eigenvalue is positive, we derive the following estimate for the separation between the interfaces of the u and v fronts in the limit as the principle eigenvalue tends to zero.

Corollary 1. *Suppose that there exists a one-parameter family of $g_\eta(u)$ such that the principle eigenvalue of H_{g_η} is η. For all $\delta > 0$ there exists $\eta_0(\delta) > 0$ so that for all $0 < \eta < \eta_0$ there exists an interval $I_\eta(\delta)$ such that the traveling fronts from Theorem 1 satisfy*

$$|(U_{KPP}(\xi), V(\xi)) - (1, 0)| < \delta \quad \text{for} \quad \xi \in I_\eta,$$

with $|I_\eta| = -\Delta \log(\eta)(1 + o(1))$, with

$$\Delta = \begin{cases} \frac{d}{2-2\sqrt{1-dg(1)}} & \text{if} \quad dg(1) < \frac{3}{4} \\ \frac{d}{2\sqrt{1-dg(1)}} & \text{if} \quad dg(1) > \frac{3}{4} \end{cases} . \tag{2.4}$$

Remark 1. *The techniques used in the proof of Theorem 1 and Corollary 1 generalize to more complicated systems and do not rely on the decoupling of the u component or the existence of a comparison principle for (1.1). We expect that our techniques could be applied to systems of the form (1.2) to show the existence of locked fronts. In addition, the method of proof naturally provides estimates for the front separation depending on the resonance structure of the eigenvalues of the fixed point corresponding to the intermediate state. The primary simplification in passing from (1.2) to (1.1) is the invariance of the system with $u = 1$. This*

invariance simplifies the analysis of the front connecting the stable and intermediate state to that of the well known Nagumo front. The primary challenge in extending these results is understanding the precise nature of the traveling front connecting these two states as well as dealing with more complicated nonlinearities. We give an example in Appendix A of a system where the nonlinearities play an important role in the speed selection.

Remark 2. *It is perhaps tempting to view the locked front as a pulled front in an inhomogeneous medium, but this analogy is not entirely complete. When the leading eigenvalue of H_g is positive, compactly supported perturbations of the $v = 0$ steady state will spread with asymptotic speed greater than two in the linear equation. However, the maximum observed speed of propagation is two and no faster. This implies that the speed of propagation of the v component can not necessarily be determined directly from the linear spreading speed of the equation $u_t = H_g u$. In addition, this implies that the linear spreading speed in this inhomogeneous medium does not place a lower bound on the spreading speed for the full system.*

When the principle eigenvalue of H_g is negative, we expect that these two fronts no longer lock. Nonetheless, one can still ask what the selected wavespeed for the v component is. Recall that when the leading eigenvalue is negative, then the spreading speed induced by the KPP front is less than the speed of the KPP front itself. One might expect this speed to only be observed transiently with the speed eventually relaxing to the asymptotic rate of the state $u = 1$ in the wake. However, this is not always what is observed – as we pointed out in Figure 1. We provide the following argument as to why this might be expected. As the KPP front propagates through the medium, this front alters the natural rate of decay for the v component. When these decay rates are weaker than the decay rate selected by the state in the wake, then faster speeds of propagation may be observed. Using the leading eigenvalue, we provide an estimate for this invasion speed that corresponds well with numerical experiments.

Rigorous analysis of this case is more complicated. The dynamics evolve on two different time scales, which means that for no choice of traveling coordinate are the dynamics stationary. Due to these complications the dynamical system approach is no longer applicable and we turn to comparison techniques. We establish that the selected wavespeed for the v component is equal to our prediction. To do this, we must make one additional technical assumption on the inhomogeneity; that is we require $g'(1) < 0$.

Theorem 2. *Assume A1 and A2 above. Suppose $g'(1) < 0$. Fix $d > 0$ and $g(u)$ and define*

$$\lambda = \sup_{\omega \in \sigma(H_g)} \omega.$$

Consider initial data, $0 \leq u_0(x) \leq 1$, and $0 \leq v_0(x) \leq \sqrt{g(1)}$, both compactly supported perturbations of a Heaviside step function. Define the invasion point,

$$\delta(t) := \sup_{x \in \mathbb{R}} \left\{ x \mid v(t,x) \geq \frac{\sqrt{g(1)}}{2} \right\}.$$

If $\lambda \in (2(g(1) - \sqrt{g(1)/d}), 0)$, then the selected wavespeed for the v component, defined as $\lim_{t\to\infty} \delta(t)/t$, is equal to

$$s_v = 2 - \frac{d\lambda}{-1 + \sqrt{1 - dg(1) + d\lambda}}.$$

Remark 3. *We emphasize that the existence of accelerated fronts is not an artifact of the decoupling of the u component from the v component. As in the locked case, we expect this behavior to be observed in a number of staged invasion processes, including (1.2) for example. In contrast to the locked case, extending the rigorous analysis to more general systems is not straightforward. The proof of Theorem 2 relies on both the comparison structure and the decoupling of the u component. Extending the analysis to systems lacking these two properties will require new techniques. On the other hand, in more general systems the linearization about the primary front and, in particular, the location of resonance poles would provide an estimate for the spreading speed of the secondary front in a manner analogous to the analysis in this article. We would expect this estimate to be reliable in a number of examples.*

3 The locked case: proof of Theorem 1

Our approach is to first consider the case when the principle eigenvalue is near zero. In this limit, we show the existence of a traveling front solution using a geometric approach. That is, we will prove Corollary 1 first and then subsequently extend the existence result to parameter values that lead to larger principle eigenvalues.

To begin, we will consider a one parameter family of inhomogeneities $g_\eta(u)$, parameterized by their leading eigenvalue, i.e. η is the leading eigenvalue of H_{g_η}. We consider small η for the time being.

We fix some notation first. Define,

$$\tilde{\mathrm{P}}_u := (0,0), \quad \tilde{\mathrm{P}}_i := (1,0), \quad \tilde{\mathrm{P}}_s := (1, \sqrt{dg(1)}),$$

as the unstable, intermediate and stable homogeneous states, respectively. We will seek traveling front solutions to the system (1.1), connecting the homogeneous state $\tilde{\mathrm{P}}_s$ to $\tilde{\mathrm{P}}_u$ via the intermediate state $\tilde{\mathrm{P}}_i$. To do so, we work in a moving coordinate frame $\xi = x - 2t$ and seek stationary solutions in this frame, i.e solutions satisfying,

$$\begin{aligned} 0 &= u_{\xi\xi} + 2u_\xi + u(1-u) \\ 0 &= dv_{\xi\xi} + 2v_\xi + g(u)v - v^3, \end{aligned}$$

subject to the condition that $(u(\xi), v(\xi))$ tends to P_u as $\xi \to \infty$ and to P_s as $\xi \to -\infty$. Expand this system of second order equations into a system of first order equations,

$$\begin{aligned} u_1' &= u_2 \\ u_2' &= -2u_2 - u_1(1-u_1) \\ v_1' &= v_2 \\ v_2' &= d^{-1}(-2v_2 - g(u_1)v_1 + v_1^3). \end{aligned} \tag{3.1}$$

This system has three fixed points of interest, $\mathrm{P}_{u,i,s}$, the natural analogs of the homogeneous states $\tilde{\mathrm{P}}_{u,i,s}$. As is usually the case with invasion fronts, the fixed point P_s is a saddle with two dimensional stable and unstable manifolds while the fixed point P_u is a stable node with a four dimensional stable manifold. To select a unique front, we note that the subspace with $v_1 = v_2 = 0$ is invariant and the selected front for this subsystem is known to be the Fisher-KPP front $U_{KPP}(\xi)$. Furthermore, the linearization at P_u transverse to this subspace has a spectral gap between the weak stable and strong stable eigenvalues. As a consequence, there exists a strong stable manifold of this trajectory and we seek traveling front solutions lying in this two dimensional manifold. That is, we seek intersections of the manifolds

$$\mathcal{M}^- := W^u(\mathrm{P}_s), \quad \mathcal{M}^+ := W^{ss}(U_{KPP}(\xi)).$$

The subspace with $u_1 = 1$ and $u_2 = 0$ is also invariant and the dynamics in this subspace reduce to a rescaled version of Nagumo's equation. This equation admits monotone traveling front solutions for all speeds greater than $2\sqrt{dg(1)}$ that connect the stable and intermediate states. We will use this front, along with the KPP front as a skeleton by which to track the evolution of the above manifolds. That is, we track $\mathcal{M}^-$ forward into a neighborhood of P_i, track $\mathcal{M}^+$ backwards along the KPP front into a neighborhood of P_i and then use a local analysis about P_i to derive conditions leading to an intersection of these two manifolds. See Figure 2.

For convenience, we assume that $g(1)$ is independent of η, although that is not necessary for the result. We focus on the dynamics near P_i. We compute the linearization at P_i, which has the eigenvalues,

$$\nu_u^\pm = -1 \pm \sqrt{2}, \quad \nu_v^\pm = -\frac{1}{d} \pm \frac{\sqrt{1 - dg(1)}}{d}.$$

Here $\nu_u^- < 0 < \nu_u^+$ denote the eigenvalues governing the dynamics in the $v = 0$ subspace while $\nu_v^- < \nu_v^+ < 0$ govern the dynamics in the $u = 1$ invariant subspace.

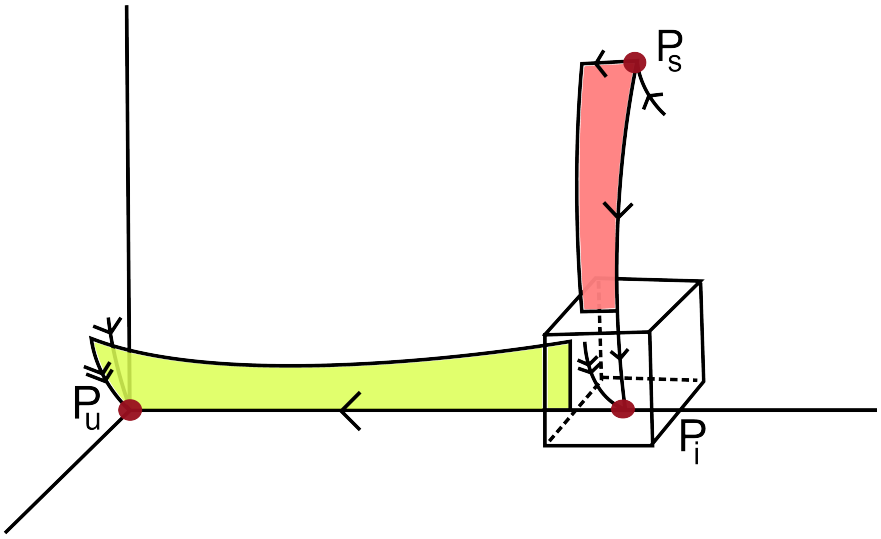

Figure 2: A schematic outlining the method of proof of Theorem 1. Traveling front solutions exist that connect the fixed points P_s and P_i (the Nagumo front) as well as P_i and P_u (the KPP front). These fronts are used as a skeleton by which to track $\mathcal{M}^{\pm}$ to a neighborhood of P_i. A local analysis of this fixed point allows for a comparison of these two manifolds.

Normal form analysis near P_i. The first order of business is to introduce a change of coordinates that brings a neighborhood of the fixed point P_i into a form suitable for treatment via Shilnikov's approach, see [21, 9]. Shilnikov's idea is to study the dynamics near P_i not as an initial value problem but as a boundary value problem taken over an asymptotically large ξ interval. The boundary data for the contracting coordinates are prescribed at $\xi = 0$ while the boundary data for the expanding coordinates are prescribed at $\xi = T$ for $T \gg 1$. Solutions to this boundary value problem describe orbits that are asymptotically close to the intermediate state P_i over an asymptotically large interval of ξ values. In fact, we can change coordinates in such a way as to gain explicit asymptotic expansions for this solution near its entry and exit from the neighborhood of P_i. It is these asymptotic expansions that we will use to compare the manifolds $\mathcal{M}^{\pm}$.

To elucidate the underlying asymptotics, we must make several changes of variables. The techniques used to construct this change of coordinates are standard, see for example [16]. However, these coordinates play an important role in the asymptotics that will be derived so we outline them here. We first diagonalize the linearization about P_i. That is, we introduce coordinates $(\tilde{y}_1, \tilde{x}_1, \tilde{x}_2, \tilde{x}_3)$, with

$$\begin{aligned}
\tilde{y}_1 &= \frac{1}{\nu_u^- - \nu_u^+}\left(\nu_u^- \tilde{u}_1 - u_2\right) \\
\tilde{x}_1 &= \frac{1}{\nu_u^- - \nu_u^+}\left(-\nu_u^+ \tilde{u}_1 + u_2\right) \\
\tilde{x}_2 &= \frac{1}{\nu_v^- - \nu_v^+}\left(\nu_v^- v_1 - v_2\right) \\
\tilde{x}_3 &= \frac{1}{\nu_v^- - \nu_v^+}\left(-\nu_v^+ v_1 + v_2\right),
\end{aligned}$$

where $\tilde{u}_1 = u_1 - 1$. This diagonalizes the linear part, leaving

$$\begin{aligned}
\tilde{y}_1' &= \nu_u^+ \tilde{y}_1 - \frac{(\tilde{x}_1 + \tilde{y}_1)^2}{\nu_u^- - \nu_u^+} \\
\tilde{x}_1' &= \nu_u^- \tilde{x}_1 + \frac{(\tilde{x}_1 + \tilde{y}_1)^2}{\nu_u^- - \nu_u^+} \\
\tilde{x}_2' &= \nu_v^+ \tilde{x}_2 + \frac{g_1(\tilde{x}_1, \tilde{y}_1, \eta)}{d(\nu_v^- - \nu_v^+)}(\tilde{x}_2 + \tilde{x}_3) - \frac{(\tilde{x}_2 + \tilde{x}_3)^3}{\nu_v^- - \nu_v^+} \\
\tilde{x}_3' &= \nu_v^- \tilde{x}_3 - \frac{g_1(\tilde{x}_1, \tilde{y}_1, \eta)}{d(\nu_v^- - \nu_v^+)}(\tilde{x}_2 + \tilde{x}_3) + \frac{(\tilde{x}_2 + \tilde{x}_3)^3}{\nu_v^- - \nu_v^+}.
\end{aligned} \tag{3.2}$$

Here $g_1(\tilde{x}_1, \tilde{y}_1)$ is $g_\eta(u_1) - g_\eta(1)$ expressed in $(\tilde{x}_1, \tilde{y}_1)$ coordinates. We then make the following nonlinear changes of coordinates.

Lemma 3.1. *There exists a smooth change of coordinates $\Phi_1 : \mathbb{R}^4 \to \mathbb{R}^4$ so that system (3.2) is reduced to*

$$\begin{aligned}
y_1' &= \nu_u^+ y_1 + y_1 N_y(y_1, x_1) \\
x_1' &= \nu_u^- x_1 + x_1 N_1(y_1, x_1) \\
x_2' &= \nu_v^+ x_2 + x_2 \gamma_1(y_1, x_1) + x_3 \gamma_2(y_1, x_1) + N_2(y_1, x_1, x_2, x_3) \\
x_3' &= \nu_v^- x_3 + x_2 \gamma_3(y_1, x_1) + x_3 \gamma_4(y_1, x_1) + N_3(y_1, x_1, x_2, x_3),
\end{aligned} \tag{3.3}$$

for some functions $N_{2,3}$ with local Taylor expansions,

$$N_{i=2,3} = \sum_{|\alpha| \geq 3} \gamma_{\alpha,i}(y_1, x_1) x_2^{\alpha_1} x_3^{\alpha_2} e_i.$$

Here $|\alpha| \geq 3$ since the nonlinearity is cubic.

Proof: The stable and unstable manifolds of P_i are smooth, and coordinates can be chosen so that these manifolds coincide with the subspaces $y_1 = 0$ (for the stable manifold) and $x_i = 0$ (for the unstable manifold).

■

Note that in our example, the $x_1 - y_1$ subspace decouples. The unstable manifold comprises the KPP front and therefore the only trajectory in the $x_1 - y_1$ subspace that is of interest is the unstable manifold itself. Having straightened the stable and unstable manifolds, we can safely restrict to the subspace with $x_1 = 0$. We will henceforth disregard the dependence of the vector field upon x_1.

To find traveling front solutions, we will need detailed information on the evolution of solutions as they pass near the fixed point P_i. To do this, we use variation of parameters and write out the integral equations for the evolution of x_2 and x_3,

$$\begin{aligned}
x_2(\xi) &= e^{\nu_v^+ \xi} x_2(0) + \int_0^\xi e^{\nu_v^+ (\xi - \sigma)} \left(x_2(\sigma)\gamma_1(y_1(\sigma)) + x_3(\sigma)\gamma_2(y_1(\sigma)) + N_2(y_1(\sigma), x_2(\sigma), x_3(\sigma)) \right) d\sigma \\
x_3(\xi) &= e^{\nu_v^- \xi} x_3(0) + \int_0^\xi e^{\nu_v^- (\xi - \sigma)} \left(x_2(\sigma)\gamma_3(y_1(\sigma)) + x_3(\sigma)\gamma_4(y_1(\sigma)) + N_3(y_1(\sigma), x_2(\sigma), x_3(\sigma)) \right) d\sigma
\end{aligned} \tag{3.4}$$

By imposing boundary data for the y_1 component at $\xi = T$, the solution $y_1(\xi)$ is bounded for $\xi \in [0, T]$ and this eliminates growing exponential terms from the integral equations for the evolution of x_2 and x_3. With this formulation the existence of a bounded solution to these integral equations can be readily shown, however we will need more. In particular, we would like to have some sharp asymptotics for the x_2 and x_3 solutions as they exit a neighborhood of the origin in the limit as $T \to \infty$. To accomplish this, various other terms must be removed. For example, the x_2 component will evolve to leading order like its linearization provided that the $x_2\gamma_1(y_1)$ term is removed. One might hope for the same property in x_3 after removing the term $x_3\gamma_4(y_1)$ from that equation. As it turns out, the situation here is more complicated and the leading order asymptotics for the x_3 component depend on the the relationship between the eigenvalues $\nu_v^\pm$ and the nonlinearity N_3. We have the following.

Lemma 3.2. *Consider the vector field (3.3). There exists a rescaling of the independent variable and a smooth change of coordinates $\Phi_2 : \mathbb{R}^4 \to \mathbb{R}^4$ that transforms (3.3), restricted to $x_1 = 0$, to the following system,*

$$\begin{aligned} y_1' &= \nu_u^+ y_1 \\ x_2' &= \nu_v^+ x_2 + \gamma_2(y_1) x_3 + \tilde{N}_2(y_1, x_2, x_3) \\ x_3' &= \nu_v^- x_3 + \tilde{N}_3(y_1, x_2, x_3), \end{aligned} \tag{3.5}$$

in a neighborhood of P_i*, for some* $\tilde{N}_i$ *with* $|\tilde{N}_i| < C_i(|x_2| + |x_3|)^3$.

Proof: With $x_1 = 0$, the nonlinear equation for y_1 can be linearized through a y_1 dependent rescaling of the independent variable. This introduces new nonlinear terms on the right hand side of (3.3) which we absorb into the coefficients γ_i and $\gamma_{\alpha,i}$. To simplify notation, we use the same coefficient functions with the understanding that they have changed. We will now perform a sequence of transformations to remove various terms in (3.3). We use techniques outlined in [16, Section 3.2]. They are as follows.

1. We begin by removing the $x_2\gamma_3(y_1)$ term from the equation for x_3. Consider the change of coordinates $\bar{x}_3 = x_3 + p(y_1)x_2$, with x_2 unchanged. Then the evolution of $\bar{x}_3$ is

   $$\bar{x}_3' = \nu_v^- \bar{x}_3 + x_2 \left(\gamma_3(y_1) + p'(y_1) - (\nu_v^- - \nu_v^+)p(y_1) + \gamma_1(y_1)p(y_1)\right).$$

   Taking p to be a new dependent variable, then the homological equation can be expressed by the system of equations,

   $$\begin{aligned} y_1' &= \nu_u^+ y_1 \\ p' &= (\nu_v^- - \nu_v^+)p - \gamma_3(y_1) - \gamma_1(y_1)p. \end{aligned}$$

   The origin of this system is a hyperbolic fixed point and for small y_1 the unstable manifold is given as a smooth graph $p = h(y_1)$, which defines the smooth change of coordinates that we require.

2. We now drop the bars from $\bar{x}_3$. Similarly, we note that this change of coordinates alters the coefficients $\gamma_i(y_1)$. We continue to use the same coefficient functions with the understanding that they have changed.

   We then turn our attention to removing terms of the form $x_2\gamma_1(y_1)$ from the equation for x_2. First remove any quadratic terms in $x_2 y_1$ via a normal form coordinate change. We then proceed as above. Consider a change of coordinates of the form $\bar{x}_2 = x_2 + p(y_1)x_2$. In the new coordinates, we have,

   $$\bar{x}_2' = \nu_v^+ \bar{x}_2 + \bar{x}_2 \left(\frac{\gamma_2(y_1) + p'(y_1)}{1 + p(y_1)}\right) + h.o.t..$$

   Using p as a new coordinate we require,

   $$p' = -\gamma_2(y_1), \quad y_1' = \nu_u^+ y_1.$$

   As was the case for the previous change of coordinates, the origin has a smooth unstable manifold whose graph gives the desired change of coordinates.

3. A similar change of coordinates removes terms of the form $x_3\gamma_3(y_1)$ from the equation for x_3.

Following these changes of variables, the system (3.1) reduces to (3.5).

■

We will now use Shilnikov's approach to analyze solutions of (3.5), [21, 9]. We seek solutions to the boundary value problem with boundary conditions $y_1(T) = y_1^{out}$, $(x_2, x_3)(0) = (x_2^{in}, x_3^{in})$ for some $T \gg 1$. To be precise, let $\delta > 0$ and define the entrance and exit sections,

$$\Sigma^{in} := \{(y_1, x_1, x_2, x_3) \mid x_2 = \delta\}, \quad \Sigma^{out} := \{(y_1, x_1, x_2, x_3) \mid y_1 = \delta\}.$$

Let $\pi : \Sigma^{in} \to \Sigma^{out}$ be the corresponding transition map. We have the following result.

Lemma 3.3. *For any x_3^{in} sufficiently small and any $T \gg 1$, there exists a unique solution to (3.5) originating in Σ^{in} at $\xi = 0$ and evolving to Σ^{out} with $\xi = T$. This solution has the following asymptotics,*

$$\begin{aligned} y_1(0) &= e^{-\nu_u^+ T}\delta \\ x_2(T) &= e^{\nu_v^+ T}x_2^{in} + \mathcal{O}(e^{(\nu_v^+ - \omega)T}) \\ x_3(T) &= \mathcal{O}(e^{(\nu_v^+ - \omega)T}), \end{aligned} \tag{3.6}$$

for some $\omega > 0$. The asymptotics for $x_3(T)$ can be improved depending on the nonlinearity and the ratio of the relevant eigenvalues. We have

$$\begin{aligned} x_3(T) &= e^{\nu_v^- T}x_3^{in} + \mathcal{O}(e^{(\nu_v^- - \omega)T}) \quad \text{if} \quad 3\nu_v^+ - \nu_v^- < 0 \\ x_3(T) &= e^{3\nu_v^+ T}\frac{(x_2^{in})^3}{(3\nu_v^+ - \nu_v^-)(\nu_v^- - \nu_v^+)} + \mathcal{O}(e^{(3\nu_v^+ - \omega)T}) \quad \text{if} \quad 3\nu_v^+ - \nu_v^- > 0. \end{aligned} \tag{3.7}$$

Proof: The y_1 solution is explicit and the existence of a solution for the x_2 and x_3 components can be shown using the contraction mapping theorem applied to (3.4) on the space, $C^0([0,T],\mathbb{R}^2)$, with norm,

$$||(x_2, x_3)|| := \max \sup_{0 \le t \le T} \{|x_2(t)|e^{-\nu_v^+ t}, |x_3(t)|e^{-(\nu_v^+ - \omega)t}\},$$

for some $\omega > 0$. The asymptotics in (3.7) may also be derived in the process.

■

We now turn our attention to the manifolds $\mathcal{M}^-$ and $\mathcal{M}^+$. In order to apply Lemma 3.3 we will need expansions for these manifolds within the sections Σ^{in} and Σ^{out}, respectively. We begin with the expansion for $\mathcal{M}^-$.

We first fix $\delta > 0$ so that the sections Σ^{in} and Σ^{out} intersect the neighborhood of zero for which the changes of coordinates $\Phi_{1,2}$ are valid.

Lemma 3.4. *The manifold $\mathcal{M}^-$ intersects the section Σ^{in} and the intersection can be written as the graph,*

$$x_3 = h(x_2, y_1, \eta),$$

with

$$\begin{aligned} h(x_2, y_1, \eta) &= C_- x_2^3 + c_y y_1 + r_h(x_2, y_1) \quad \text{if} \quad 3\nu_v^+ - \nu_v^- > 0 \\ h(x_2, y_1, \eta) &= C_- x_2^{\nu_v^-/\nu_v^+} + c_y y_1 + r_h(x_2, y_1) \quad \text{if} \quad 3\nu_v^+ - \nu_v^- < 0 \end{aligned}$$

for some $C_- < 0$.

Proof: In (u_1, u_2, v_1, v_2) coordinates, we note that the $u_1 = 1$, $u_2 = 0$ subspace is invariant. Here the traveling wave equation for the v dynamics reduces to a rescaled version of Nagumo's equation. Traveling front solutions exist for all wavespeeds greater than the linear spreading speed, in this case $2\sqrt{dg(1)}$. The linear spreading speed is the selected speed for this particular scaling of Nagumo's equation. Thus, any front that propagates faster necessarily approaches P_i along the weaker of the two possible eigendirections.

Transforming into the (y_1, x_2, x_3) coordinates, an expansion for this trajectory can be computed via normal form theory. We remark that the weak-stable manifold is not unique, but all trajectories are asymptotic to the same nonlinear manifold. This manifold is finitely smooth, with the degree of smoothness prescribed by the resonances of the eigenvalues $\nu_v^\pm$. Whenever $3\nu_v^+ > \nu_v^-$ the manifold is at least C^3 and can be given as a graph,

$$x_3 = C_- x_2^3(1 + o(1)).$$

For the particular choice of nonlinearity considered in (1.1) the leading order coefficient is calculated to be,

$$C_- = \frac{1}{3\nu_v^+ - \nu_v^-}\frac{1}{\nu_v^- - \nu_v^+},$$

again provided that $3\nu_v^+ > \nu_v^-$. Note that $\text{sign}(C_-) = -\text{sign}(3\nu_v^+ - \nu_v^-) < 0$. The manifold $\mathcal{M}^-$ varies smoothly, so for $y_1 \neq 0$, this manifold is again given as a graph, $x_3 = h(x_2, y_1, \eta)$, with

$$h(x_2, y_1, \eta) = C_- x_2^3 + c_y y_1 + r_h(x_2, y_1).$$

As a result, in the section Σ^{in}, the manifold $\mathcal{M}^-$ is given locally as a graph over y_1,

$$y_1 = y_1^{in}, \quad x_2 = \delta, \quad x_3 = h(\delta, y_1^{in}, \eta). \tag{3.8}$$

Whenever $3\nu_v^+ < \nu_v^+$, then a generic weak-stable manifold will no longer be C^3, but will have an expansion with leading order terms of $x_2^{\nu_v^-/\nu_v^+}$. The determination of which of these manifolds describes the traveling Nagumo front is then a global problem. The relevant property for the analysis here is whether the front approaches the origin above or below the weak-stable eigenspace. If the front approaches from below, then converting to $x_2 - x_3$ coordinates we find a local expansion $x_3 = h(x_2)$ with $h(x_2) > 0$. We must rule out this possibility, as it will become clear later that this type of approach will lead to a subcritical bifurcation. We proceed to consider the set

$$\left\{(v_1, v_2) \in \mathbb{R}^2 | 0 < v_1 < \sqrt{g(1)}, \nu_v^+ v_1 < v_2 < 0\right\}.$$

It is easily shown that this set is a trapping region and therefore constrains the tracked manifold $\mathcal{M}^+$ to approaching the origin above the weak-stable eigenspace. As a result, whenever $3\nu_v^+ < \nu_v^-$ we can again express $\mathcal{M}^-$ as a graph over y_1 as was done above.

■

We now proceed to track $\mathcal{M}^+$ backwards to its intersection with Σ^{out}.

Lemma 3.5. *The manifold $\mathcal{M}^+$ intersects Σ^{out} and for η sufficiently small this intersection can be written as the graph*

$$x_3 = -c_\eta \eta x_2 + c_+ x_2^3 + o(x_2^3), \tag{3.9}$$

Proof: We seek a description of $\mathcal{M}^+$ near $y_1 = \delta$. There are essentially two components of this process. First, we describe $\mathcal{M}^+$ using variation of parameters. Then, we transform this description into local coordinates about P_i. Fix ξ_0 so that $\Phi_2\Phi_1(U_{KPP}(\xi_0), U'_{KPP}(\xi_0), 0, 0)) \in \Sigma^{out}$. For small v_1 and v_2, $\mathcal{M}^+$ is given by solutions to

$$0 = dv'' + 2v' + g_\eta(U_{KPP}(\xi))v - v^3, \quad v \in L^\infty_{d^{-1}}(\mathbb{R}^+). \tag{3.10}$$

We write this second order equation as a system of first order equations. Let $Q = (v_1, v_2)^T$. Then $Q' = A(\xi, \eta)Q + N(\xi, \eta, Q)$ with

$$A(\xi, \eta) = \begin{pmatrix} 0 & 1 \\ -\frac{g_\eta(U_{KPP}(\xi), \eta)}{d} & -\frac{2}{d} \end{pmatrix}, \quad N(\xi, \eta, Q) = \begin{pmatrix} 0 \\ \frac{v_1^3}{d} \end{pmatrix}.$$

The matrix $A(\xi, \eta)$ converges exponentially to $A_\pm(\eta) := \lim_{\xi \to \pm\infty} A(\xi, \eta)$. Under our assumptions above, these asymptotic matrices possess a spectral gap between their strong and weak stable eigenvalues. As a result, the linear equation has a generalized exponential dichotomy on $\mathbb{R}^+$ with strong stable projection $P^+(\xi)$. Bounded solutions to the nonlinear equation (3.10) in $L^\infty_{d^{-1}}(\mathbb{R}^+)$ are given by fixed points of the following map,

$$TQ = \Omega(\xi, \xi_0)P^+(\xi_0)Q + \int_{\xi_0}^{\xi} \Omega(\xi, s)P^+(s)N(s, \eta, Q(s))ds - \int_{\xi}^{\infty} \Omega(\xi, s)(I - P^+(s))N(s, \eta, Q(s))ds, \tag{3.11}$$

where $\Omega(\xi, \xi_0)$ is the fundamental matrix solution to the linear equation $Q' = A(\xi)Q$. It is readily observed that (3.11) is a contraction mapping with a unique fixed point for each specified $Q_+(\xi_0) \in \text{Rg}(P^+(\xi_0))$. For v sufficiently small, $\mathcal{M}^+$ can be written as a graph over the range of the stable projection,

$$\mathcal{M}^+ \cap \Psi^{-1}(\Sigma^{out}) = \left\{\phi_{ss} + \gamma(\phi_{ss}) | \quad \text{for} \quad \phi_{ss} \in Rg(P^+(\xi_0)) \quad \gamma : \text{Rg}(P^+) \to \text{Rg}(1 - P^+)\right\},$$

with

$$\gamma(\phi_{ss}) = -\int_{\xi_0}^{\infty} \Omega(\xi_0, s)(I - P^+(s))N(s, \eta, Q^*(s))ds,$$

where $Q^*(s)$ is the unique solution of the contraction mapping (3.11). Now let $\psi(\xi_0)$ be a vector orthogonal to $\mathrm{Rg}(P^+(\xi_0))$. Then the nonlinear expansion of the manifold $\mathcal{M}^+$ can be expressed as a Melnikov type integral using,

$$\begin{aligned} \langle \psi(\xi_0), \gamma(\phi_{ss}) \rangle &= -\int_{\xi_0}^{\infty} \langle \psi(\xi_0), \Omega(\xi_0, s)(I - P^+(s))N(s, \eta, Q^*(s)) \rangle ds \\ &= -\int_{\xi_0}^{\infty} \langle \psi(s), N(s, \eta, Q^*(s)) \rangle ds. \end{aligned} \tag{3.12}$$

Here $\psi(s)$ is the evolution of $\psi(\xi_0)$ under the adjoint equation $\psi' = -A^T(\xi, \eta)\psi$.

When $\eta = 0$, we have $Q^*(\xi, 0, 0) = \chi e^{-d^{-1}\xi}(\phi_0(\xi), \phi_0'(\xi))$, where ϕ_0 is the eigenfunction for H_{g_0} and χ is some positive constant. Since zero is the leading eigenvalue of a Sturm-Liouville operator we can take $\phi_0 > 0$. Using the maximum principle together with the fact that $g(u) > 0$ a simple argument by contradiction establishes that $(e^{d^{-1}\xi}\phi_0)' < 0$ for all ξ. To use (3.12) we must select an orientation for $\psi(\xi)$ and since $(\psi(\xi), \psi'(\xi)) \perp (\phi_0(\xi), \phi_0'(\xi))$, we elect to consider $\psi(\xi)$ in the positive quadrant at $\eta = 0$. This implies that,

$$\langle \psi(\xi_0), \gamma(\phi_{ss}) \rangle = -\chi^3 \int_{\xi_0}^{\infty} \begin{pmatrix} \psi_1(\tau) \\ \psi_2(\tau) \end{pmatrix} \cdot \begin{pmatrix} 0 \\ d^{-1}(e^{-d^{-1}\xi}\phi_0(\tau))^3 \end{pmatrix} d\tau < 0. \tag{3.13}$$

This provides a qualitative picture of the manifold $\mathcal{M}^+$ within the section Σ^{out}. This description is accurate, not only for $\eta = 0$, but also by continuity for η small as well. It remains to transform this description into $x_2 - x_3$ coordinates so as to compute intersections with the manifold $\mathcal{M}^-$. The key remaining task is to find a description of the range of $P^+(\xi_0)$ in these new coordinates.

For small values of η, the key tool that we will use to track the tangent space is the Evans function, see for example [1]. Consider the linearized eigenvalue problem $dv'' + 2v' + g_\eta(U_{KPP})v = \lambda v$. For $\lambda = 0$, this gives the evolution of the tangent space of $\mathcal{M}^+$ under the variational equation about $U_{KPP}(\xi)$. Similar to the above analysis, we expand this equation into a non-autonomous system of first order equations, $Q' = A(\xi, \eta, \lambda)Q$ with

$$Q = \begin{pmatrix} v_1 \\ v_2 \end{pmatrix}, \quad A(\xi, \eta, \lambda) = \begin{pmatrix} 0 & 1 \\ -\frac{g_\eta(U_{KPP}(\xi), \eta)}{d} + \frac{\lambda}{d} & -\frac{2}{d} \end{pmatrix}. \tag{3.14}$$

The asymptotic matrices $\lim_{\xi \to \pm\infty} A(\xi, \lambda, \eta)$ are both stable, but working in L^2_σ with $\sigma = d^{-1}$ they can be made hyperbolic by instead considering the system $Q' = \left(A(\xi, \eta, \lambda) + d^{-1}I\right)Q$, or

$$\begin{pmatrix} v_1' \\ v_2' \end{pmatrix} = \begin{pmatrix} \frac{1}{d} & 1 \\ -\frac{g(U(\xi), \eta)}{d} + \frac{\lambda}{d} & -\frac{1}{d} \end{pmatrix} \begin{pmatrix} v_1 \\ v_2 \end{pmatrix}. \tag{3.15}$$

Since the limiting equations are hyperbolic and the non-autonomous system converges exponentially to its limiting value, there exist unique bounded solutions, $Q^\pm(\xi, \lambda, \eta)$ on both $\mathbb{R}^\pm$. The same holds true for the adjoint equation, $\Psi' = -A^*(\xi, \eta, \lambda)\Psi$, and the Evans function can be defined as,

$$D_\eta(\lambda) = Q^+(\xi, \lambda, \eta) \cdot \Psi^-(\xi, \lambda, \eta).$$

We collect some properties of D_η. It is independent of ξ. The Evans function is zero at λ if and only if λ is an eigenvalue. The existence of a simple principle eigenvalue at $\lambda = \eta$ implies that $D_\eta(\eta) = 0$ and $D_\eta'(\eta) \neq 0$. In addition, $D_\eta(\lambda)$ is analytic and as such $D_\eta(0) = C_\eta\eta + \mathcal{O}(\eta^2)$ for some value of C_η. The sign of C_η depends on the orientation chosen for the adjoint solution $\Psi^-(\xi, \lambda, \eta)$. As we did above, for large λ we expect to find everywhere positive solutions of the second order eigenvalue problem that are monotonically decreasing. We take Ψ^- to also have an everywhere positive first component for λ large. We then have $C_\eta > 0$. $D_\eta(0)$ is constructed from solutions of the original variational equation and its adjoint equation. In particular, we are interested in $Q^+(\xi, 0, \eta)$ for ξ so that $\Phi_2\Phi_1(U(\xi), U'(\xi), 0, 0) \in \Sigma^{out}$.

An important feature for the analysis here is that D_η is invariant under non-autonomous linear transformations as well as re-scalings of the independent variable. We mimic the change of coordinates above that maps the (v_1, v_2) system to the non-autonomous system

$$\begin{aligned} x_2' &= \nu_v^+ x_2 + \gamma_2(y_1)x_3 + \tilde{N}_2(y_1, x_2, x_3) \\ x_3' &= \nu_v^- x_3 + \tilde{N}_3(y_1, x_2, x_3). \end{aligned}$$

Linearizing and transforming to the weighted space yields system (3.15) in the new coordinates,

$$\begin{aligned} x_2' &= (\nu_v^+ + d^{-1})x_2 + \gamma_2(y_1)x_3 \\ x_3' &= (\nu_v^- + d^{-1})x_3. \end{aligned}$$

Any vector in span$\{(1,0)\}$ is bounded as $\xi \to -\infty$ and therefore, we see that $\Psi^-(\xi_0, 0, \eta)$ in $x_2 - x_3$ coordinates is some constant multiple of $(0,1)$. To keep the orientation consistent we take $\Psi^-(\xi_0, 0, \eta)$ to be some positive multiple of $(0,-1)$. At $\eta = 0$, there exists a bounded solution to $Q' = A(\xi, 0, 0)Q$ and therefore this solution, after transforming to local coordinates about P_i, must also be a scalar multiple of $(1,0)$ in Σ^{out}. Using the Evans function, we find that $T_y Q^+(\xi_0, 0, \eta)$ is a scalar multiple of $(1, -c_\eta \eta)$ for some constant $c_\eta > 0$. To find nonlinear corrections to this manifold we use (3.13), which after transformation to local coordinates gives $\mathcal{M}^+$ in Σ^{out} as a graph,

$$x_3 = -c_\eta \eta x_2 + c_+ x_2^3 + o(x_2^3),$$

for some $c_+ > 0$.

■

The expansions derived in Lemma 3.4 and Lemma 3.5, combined with the asymptotics of the transition map in (3.7) will allow us to show the existence of a traveling front solution with steep exponential decay in the v component when η is small.

Lemma 3.6. *For all $\eta > 0$ and sufficiently small the manifolds $\mathcal{M}^-$ and $\mathcal{M}^+$ have a non-trivial intersection.*

Proof: Let $\rho = e^{\nu_v^+ T}$. The manifold $\mathcal{M}^- \cap \Sigma^{in}$ was given as a graph in (3.8). For sufficiently large T (small ρ), the transition map π maps this graph to a graph in Σ^{out} with asymptotics as in (3.7). This transition depends qualitatively on the relationships between the eigenvalues $\nu_v^\pm$. Let $\beta = \nu_v^-/\nu_v^+$. We find two different regimes. When $\beta > 3$, then we have $3\nu_v^+ - \nu_v^- > 0$ and vice versa.

Case 1: $\beta > 3$

There exists ω_2, ω_3, both positive as well as bounded functions $r_i(\rho, \delta)$ so that $\pi\mathcal{M}^- \in \Sigma^{out}$ can be expressed as the graph

$$\begin{aligned} x_2(\rho) &= \rho\delta + \rho^{1+\omega_2} r_2(\rho, \delta) \\ x_3(\rho) &= \rho^3 \frac{\delta^3}{(3\nu_v^+ - \nu_v^-)(\nu_v^- - \nu_v^+)} + \rho^{\beta+\omega_3} r_3(\rho, \delta), \end{aligned}$$

using (3.6) and (3.8). In turn, whenever these expressions satisfy (3.9) then there exists an intersection of $\mathcal{M}^-$ and $\mathcal{M}^+$ in Σ^{out}. This condition reduces the problem to finding solutions of the equation,

$$\rho^3 \frac{\delta^3}{(3\nu_v^+ - \nu_v^-)(\nu_v^- - \nu_v^+)} + \rho^{1+\omega_3} r_3(\rho, \delta) = -c_\eta \eta(\rho\delta + \rho^{1+\omega_2} r_2(\rho, \delta)) + c_+(\rho\delta + \rho^{1+\omega_2} r_2(\rho, \delta))^3,$$

for small $\rho > 0$. Rearranging, we have

$$c_\eta \eta = c_+(\rho\delta + \rho^{1+\omega_2} r_2(\rho, \delta))^2 - \frac{\rho^3 \frac{\delta^3}{(3\nu_v^+ - \nu_v^-)(\nu_v^- - \nu_v^+)} + \rho^{3+\omega_3} r_3(\rho, \delta)}{\rho\delta + \rho^{1+\omega_2} r_2(\rho, \delta)}.$$

We factor the right hand side,

$$c_\eta \eta = \rho^2 \delta^2 \left(c_+ - \frac{1}{(3\nu_v^+ - \nu_v^-)(\nu_v^- - \nu_v^+)} + \rho^\kappa R(\rho, \delta) \right),$$

for $\kappa = \min\{\omega_2, \omega_3\}$. Rescaling $\eta = \rho^2\eta_0$, the implicit function theorem provides a solution for

$$\eta_0(\rho,\delta) = \frac{c_+\delta^2}{c_\eta} + \frac{\delta^2}{(3\nu_v^+ - \nu_v^-)(\nu_v^+ - \nu_v^-)} + \mathcal{O}(\rho^\kappa).$$

After rearranging the second term in the denominator and noting that $\beta > 3$ is equivalent to $3\nu_v^+ - \nu_v^- > 0$, we observe that local solutions exist only for $\eta > 0$.

Case 2: $\beta < 3$

We now consider $\beta < 3$. Again, there exists constants ω_2, ω_3 both positive as well as bounded functions $r_i(\rho,\delta)$ so that the manifold $\mathcal{M}^-$ in the section Σ^{out} is described by the expressions,

$$\begin{aligned} x_2(\rho) &= \rho\delta + \rho^{1+\omega_2} r_2(\rho,\delta) \\ x_3(\rho) &= \rho^\beta x_3^{in} + \rho^{\beta+\omega_3} r_3(\rho,\delta). \end{aligned}$$

Recall that x_3^{in} is given by (3.8), for which we have $x_3^{in} = C_-\delta^\beta(1+\mathcal{O}(\delta))$. The constant C_- was shown to be always negative. Again using (3.9), we find that local intersections of the manifolds $\mathcal{M}^+$ and $\mathcal{M}^-$ occur only if

$$\rho^\beta x_3^{in} + \rho^{\beta+\omega_3} r_3(\rho,\delta) = -c_\eta\eta\left(\rho\delta + \rho^{1+\omega_2} r_2(\rho,\delta)\right) + c_+\left(\rho\delta + \rho^{1+\omega_2} r_2(\rho,\delta)\right)^3.$$

The lowest order term is now $\rho^{\beta-1}$ and factoring we find the bifurcation equation,

$$c_\eta\eta = \rho^{\beta-1}\left(-\frac{x_3^{in}}{\delta} + \rho^\kappa R(\rho,\delta)\right),$$

where $\kappa = \min\{3-\beta, \omega_3\}$. Rescaling $\eta = \eta_\beta\rho^{\beta-1}$ and substituting, $x_3^{in} = C_-\delta^3 + c_y y_1^{in} + R_\delta(\delta)$, where $y_1^{in} = \delta e^{-\nu_u^+ T} = \delta\rho^{-\nu_u^+/\nu_v^+}$ we have the equivalent form,

$$c_\eta\eta_\beta = -C_-\delta^{\beta-1} + R_\delta(\delta) + \rho^{\tilde\kappa}\tilde R(\rho,\delta),$$

for $\tilde\kappa = \min\{\kappa, \frac{-\nu_u^+}{\nu_v^+}\}$. Again, the implicit function theorem gives a solution

$$\eta_\beta(\rho,\delta) = \frac{-C_-\delta^2 + R_\delta(\delta)}{c_\eta} + \mathcal{O}(\rho^{\tilde\kappa}).$$

Since $C_- < 0$, we find that the bifurcation is again supercritical and there exists a locked solution for $\eta > 0$ and sufficiently small.

■

Proof of Corollary 1 We have now established the existence of a locked fronts for the principle eigenvalue of H_g positive and small. In addition, the above analysis provides an asymptotic expansion for the distance between the interfaces of the locked front and the KPP front. In between these interfaces, the system will be quenched into the unstable intermediate state $\tilde{\mathrm{P}}_i$. In terms of the dynamic construction above, the distance between front interfaces is the transition "time" in ξ for which the locked front trajectory lies in the a neighborhood of the intermediate state P_i. We first consider $\beta > 3$. The relation $\eta = \rho^2\eta_0(\rho,\delta)$ implies that

$$T = \frac{1}{2\nu_v^+}\log\eta + \mathcal{O}(1).$$

On the other hand, when $\beta < 3$, then the relation $\eta = \rho^{\beta-1}\eta_\beta(\rho,\delta)$ implies

$$T = \frac{1}{(\beta-1)\nu_v^+}\log\eta + \mathcal{O}(1).$$

Note that in the changes of coordinates above, a rescaling of the independent variable was performed,

$$\tau = \int_0^\xi \left(1 + \frac{f(y_1(s))}{\nu_u^+ y_1(s)}\right) ds.$$

Reverting to the original independent variable only introduces $\mathcal{O}(1)$ corrections to the above asymptotic expansions.

■

Conclusion of the proof of Theorem 1 We now relax our condition that the principle eigenvalue is small and consider arbitrary positive eigenvalues. We consider the traveling front system in projective coordinates (v_1, α) with $\alpha = \frac{v_2}{v_1}$. The evolution of the system in these coordinates is,

$$\begin{aligned} v_1' &= \alpha v_1 \\ \alpha' &= -\frac{g(U_{KPP}(\xi))}{d} - \frac{2}{d}\alpha - \alpha^2 + \frac{v_1^2}{d}. \end{aligned}$$

We consider the shooting problem wherein the manifold $\mathcal{M}^-$ is transformed to projective variables and tracked as it evolves between $u = 1$ and $u = 0$. We will show that this tracked manifold retains an intersection with the manifold $\mathcal{M}^+$. When $v_1 = 0$, we recover the dynamics for the tangent space that was studied above. That is, the tangent space at $u = 1$ gives an initial condition in projective coordinates of $(v_1, \alpha) = (0, \alpha_0)$ for some $\alpha_0 < 0$. Since the principle eigenvalue is positive, the solution with this initial condition, $(v_1(\xi), \alpha(\xi))$ satisfies $v_1(\xi) = 0$ and $\alpha(\xi)$ reaching $\alpha = -\infty$ in finite time. Physically, this shows the clockwise twisting of the manifold $\mathcal{M}^-$ about the origin in $v_1 - v_2$ space.

On the other hand, as $v_1 \to \infty$ the manifold $\mathcal{M}^-$ lies in the positive quadrant. For very large v_1, the influence of the inhomogeneity is negligible and the tracked manifold lies in the positive quadrant as u evolves from $u = 1$ to $u = 0$. This can be made precise by computing the behavior of the vector field at infinity. We omit the details of this calculation.

■

This concludes the proof of Theorem 1 and our treatment of locked fronts.

4 The accelerated case

We now turn our attention to the case when the spectrum of the operator H_g is negative. Here we do not expect locking, however, the asymptotic rate of propagation of the v front is not clear. At first glance, one might expect that this front will be a pulled front, driven by the instability of the state $(u = 1)$ in which the front interface travels. This is not entirely the case. We find a critical (negative) value of the spectral parameter, below which the v front propagates at the linear spreading speed of the state $v = \sqrt{g(1)}$ behind the wake. However, above this critical value we find that the speed of this secondary front is advanced by the leading front, even as the distance between their interfaces tends to infinity. Again, we refer the reader to Figure 1, where two distinct regimes are noticed: one where the secondary front travels with the linear spreading speed and a secondary regime where the speed of this front is accelerated.

Formal derivation of selected speed The key observation is well-known. Fronts with "weak" decay propagate faster. Consider the scalar reaction diffusion equation for v when $u = 1$,

$$v_t = dv_{xx} + g(1)v - v^3. \tag{4.1}$$

Compactly supported initial conditions give rise to a pair of counter-propagating pulled fronts traveling with speed $2\sqrt{dg(1)}$. Nonetheless, faster propagation speeds are observed for initial data that is not compactly supported, but instead decays with some slow exponential rate. A rigorous treatment can be made using Fourier-Laplace transforms, see for example [3], but we restrict ourselves to a formal argument. Consider the exponential $e^{\nu x + \lambda t}$. The dispersion relation for (4.1) is,

$$\lambda = d\nu^2 + g(1).$$

This equation relates spatial modes $e^{\nu x}$ to their temporal growth rates, λ. The dispersion relation implies that the exponential will evolve as,

$$e^{\nu x + \lambda(\nu) t} = e^{\nu x + (d\nu^2 + g(1))t} = e^{\nu(x + (d\nu + \frac{g(1)}{\nu})t}. \tag{4.2}$$

This factoring makes explicit the idea that if one moves in a frame with speed $-d\nu - \frac{g(1)}{\nu}$, then marginal stability is achieved. This speed is the selected speed for exponentially decaying initial conditions. In

particular if $-\sqrt{\frac{g(1)}{d}} < \nu < 0$, then the speed of this exponential will exceed the linear spreading speed $2\sqrt{dg(1)}$.

We return our attention to the selected speed for the v front in (1.1). The linear spreading speed $2\sqrt{dg(1)}$ clearly places a lower bound on the propagation speed. However, it is possible that the propagation of the u front through the medium prepares the data in the v component in such a way that a faster speed is selected. We derive an estimate for the selected speed.

Fix g so that the principle eigenvalue of H_g exists and is negative. We again work in the frame $\xi = x - 2t$. Associated to this eigenvalue is an eigenfunction $\phi(\xi)$, i.e. $H_g\phi = \lambda\phi$. This eigenfunction is positive, bounded and solves the nonautonomous differential equation,

$$d\phi'' + (-d^{-1} + g(U_{KPP}(\xi)) - \lambda)\phi = 0.$$

As $\xi \to -\infty$, the asymptotics of this solution are,

$$\phi(\xi) \sim Ce^{d^{-1}\sqrt{1-dg(1)+d\lambda}\xi}.$$

Transforming to the unweighted space, we expect behavior in the wake of the u front of the form,

$$v(t,\xi) \sim \phi(\xi)e^{d^{-1}\xi}e^{\lambda t} = e^{d^{-1}\sqrt{1-dg(1)+d\lambda}\xi}e^{-d^{-1}\xi}e^{\lambda t}.$$

Factoring as we did in (4.2) above, this is equivalent to $e^{\mu(s_v)(x-s_v t)}$ with

$$\begin{aligned} \mu(s_v) &= -d^{-1} + d^{-1}\sqrt{1 - dg(1) + d\lambda} \\ s_v &= 2 - \frac{d\lambda}{-1 + \sqrt{1 - dg(1) + d\lambda}}. \end{aligned} \tag{4.3}$$

What influence this behavior in the wake has on the speed of the v front remains to be seen. When this decay is steeper than the decay selected by the state in the wake, we do not expect that the speed will be advanced. However, when this decay is weaker than that of the selected front, we expect the resulting front to propagate at the faster rate corresponding to the front with exactly this same weaker decay. This critical value of λ can be calculated by finding λ so that the decay deposited in the wake, $\mu(s_v)$, is equal to the decay selected by the pulled front traveling at the linear spreading speed with $u = 1$, or $-\sqrt{d^{-1}g(1)}$. This computation yields the critical eigenvalue,

$$\lambda_{crit} = 2\left(g(1) - \sqrt{\frac{g(1)}{d}}\right).$$

We have thusfar assumed that the principle eigenvalue of H_g exists. This is not necessarily the case and it is possible that the essential spectrum constitutes the most unstable portion of the spectrum of H_g. A similar analysis applies in this context and we will show that if the supremem of the spectrum of H_g is greater than λ_{crit} then the accelerated speed is again observed.

Rigorous analysis We now have a heuristic argument as to why faster propagation is observed. We will show that initial data that is a compactly supported perturbation of a Heaviside step function will propagate with this speed. We will work out the details of the proof in the case that the rightmost point in the spectrum of H_g is an eigenvalue. To do this, we construct sub and super solutions that bound the evolution of initial conditions lying in between, see for example [11, 18]. These sub and super solutions will be shown to propagate with asymptotic speed (4.3) as $t \to \infty$ as well as to allow for steep initial data, thus justifying the claim that s_v is the selected wavespeed for this system.

We proceed in two steps. We first establish that s_v is the selected wavespeed for the scalar equation,

$$v_t = dv_{xx} + g(U_{KPP}(x - 2t))v - v^3. \tag{4.4}$$

That is, we show that initial data for the v component that is a compactly supported perturbation of a Heaviside step function will asymptotically spread with speed s_v. Next, we extend the analysis to the full system, (1.1), allowing Heaviside initial data in both the u and v components.

To fix our spatial coordinate, we will henceforth assume that $U_{KPP}(0) = 1/2$.

Lemma 4.1. *Let $g^* = \sup_{u\in[0,1]} g(u)$. Suppose $\lambda \in (\lambda_{crit}, 0)$ is the principle eigenvalue of H_g and let $\phi_\lambda > 0$ be the corresponding positive eigenfunction, unique up to scalar multiplication. Then,*

$$w(t,x) = \min\left\{\sqrt{g^*}, e^{\lambda t}\phi_\lambda(x-2t)e^{-d^{-1}(x-2t)}\right\},$$

is a super-solution.

Proof: The proof is a simple calculation. Let

$$N(v) = v_t - dv_{xx} - g(U_{KPP}(x-2t))v + v^3. \tag{4.5}$$

We compute

$$N(\sqrt{g^*}) = \sqrt{g^*}(g(U_{KPP}) - g^*) > 0,$$

and

$$\begin{aligned} N\left(e^{\lambda t}\phi_\lambda(x-2t)e^{-d^{-1}(x-2t)}\right) &= e^{\lambda t}e^{-d^{-1}(x-2t)}\left(\lambda\phi_\lambda - d\phi_\lambda'' + (d^{-1} - g(U_{KPP}(x-2t))\phi_\lambda\right) \\ &+ \left(e^{\lambda t}\phi_\lambda(x-2t)e^{-d^{-1}(x-2t)}\right)^3 \\ &= \left(e^{\lambda t}\phi_\lambda(x-2t)e^{-d^{-1}(x-2t)}\right)^3 > 0, \end{aligned}$$

establishing $w(t,x)$ as a super-solution. As $t\to\infty$, the graph of this super-solution is transported to the right with asymptotic speed s_v, given in (4.3).

■

Constructing a subsolution is more difficult. We will use the formal analysis from the beginning of this section as a guide. Namely, we suspect that, to leading order, the v dynamics are given as a concatenation of the principle eigenfunction with a traveling front solution in the wake of the KPP front that propagates with speed s_v. We construct similar subsolutions that are defined piecewise and consist of two main ingredients:

- Traveling front solutions $V_\tau(x-\sigma t)$, propagating in the medium where $u=1$ and which are solutions of (4.1). For each σ, a one parameter family of such solutions exist and we parameterize them by their location, τ, which is defined by, $V_\tau(\tau) = \sqrt{g(1)}/2$.
- Solutions to the non-autonomous ordinary differential equation,

$$\lambda\psi = d\psi'' + 2\psi' + g(U_{KPP}(\xi))\psi. \tag{4.6}$$

  Here primes are derivatives with respect to the traveling wave coordinate $\xi = x-2t$. The function $U_{KPP}(\xi)$ converges exponentially to its limiting states. It follows from standard results, see for example [7], that there exists a unique solution of (4.6) satisfying

$$\psi(\xi) = Ce^{(-d^{-1}+d^{-1}\sqrt{1-dg(1)+d\lambda})\xi}\left(1+\mathcal{O}(e^{\gamma\xi})\right) \quad \text{as } \xi\to-\infty, \tag{4.7}$$

  for some $\gamma < 0$.

Since there are two distinct time-scales in this system ($x-2t$ and $x-s_vt$) we will work in (t,x) coordinates from this point forward.

Lemma 4.2. *Let λ be the principle eigenvalue of H_g, satisfying $\lambda\in(\lambda_{crit},0)$. Suppose that $g'(1) < 0$. Consider any σ satisfying $2\sqrt{dg(1)} < \sigma < s_v$. Then, there exists an $\epsilon_0(\sigma) > 0$, $\Theta(\sigma,\epsilon_0)$ and $\tau_0(\sigma,\epsilon,\Theta)$ such that for all $0<\epsilon<\epsilon_0(\sigma)$ and all $\tau < \tau_0(\sigma,\epsilon,\Theta) < 0$ we have that*

$$z_\sigma(t,x) = \begin{cases} V_\tau(x-\sigma t) & \text{for} \quad x-2t < -\Theta \\ V_\tau((2-\sigma)t-\Theta)\tilde{\psi}_{\lambda-\epsilon}(x-2t) & \text{for} \quad x-2t \geq -\Theta, \end{cases} \tag{4.8}$$

is a subsolution for all $(t,x)\in\mathbb{R}^+\times\mathbb{R}$. Here, $\tilde{\psi}_{\lambda-\epsilon}(\cdot) := \max\{\psi_{\lambda-\epsilon}(\cdot), 0\}$, where $\psi_{\lambda-\epsilon}$ solves the ordinary differential equation in (4.6) with asymptotic boundary conditions as in (4.7) and with spectral parameter $\lambda-\epsilon$. We take $\tilde{\psi}_{\lambda-\epsilon}(-\Theta) = 1$.

In order to consolidate some formulas, we define,

$$\mu(\sigma) := -\frac{\sigma}{2d} + \frac{1}{2d}\sqrt{\sigma^2 - 4dg(1)},$$

and note that $\mu(s_v) = -d^{-1} + d^{-1}\sqrt{1 - dg(1) + d\lambda}$ and $\lambda = (2 - s_v)\mu(s_v)$, both of which may be derived from (4.3).

Proof: To begin, we select $\epsilon_0(\sigma)$ such that

$$\epsilon_0(\sigma) < \lambda - \max_{\substack{\omega \in \sigma(H_g) \\ \omega \neq \lambda}} \{\text{Re } \omega\} \tag{4.9}$$

$$\mu(\sigma) < -\frac{1}{d} + \frac{1}{d}\sqrt{1 - dg(1) + d\lambda - d\epsilon_0(\sigma)} \tag{4.10}$$

$$\epsilon_0(\sigma) < (2 - s_v)\mu(s_v) - (2 - \sigma)\mu(\sigma). \tag{4.11}$$

Both (4.10) and (4.11) are possible since $\mu(\sigma) < \mu(s_v)$. Additionally, we select $\Theta(\sigma, \epsilon_0)$ so that

$$g(U_{KPP}(\xi)) > g(1) \quad \text{for all } \ \xi < -\Theta \tag{4.12}$$

$$\mu(\sigma) < \frac{d\tilde{\psi}_{\lambda-\epsilon}}{d\xi}(-\Theta). \tag{4.13}$$

The first condition requires $g'(1) < 0$ and the second follows from (4.7) and the selection $\tilde{\psi}_{\lambda-\epsilon}(-\Theta) = 1$. It remains to show that there exists a τ_0 such that z_σ is a subsolution for all $\tau < \tau_0$. Recall that τ defines the translate of the V_τ front that is being used. Once one such front has been found, any left-translate of that front will also suffice.

Condition (4.9) together with the Sturm oscillation theorem imply that $\psi_{\lambda-\epsilon}$ has a unique zero and therefore $\tilde{\psi}_{\lambda-\epsilon}$ is positive only on a semi-infinite interval near $-\infty$.

Consider first the interval $x - 2t < -\Theta$. Recalling the definition of $N(z)$ in (4.5) we compute $N(z_\sigma)$ and find,

$$N(z_\sigma) = (g(1) - g(U_{KPP}(x - 2t))\, z_\sigma < 0,$$

establishing z_σ as a subsolution on $x - 2t < -\Theta$.

Now consider $x - 2t > -\Theta$. Whenever $z_\sigma \neq 0$, we compute

$$\begin{aligned} N(z_\sigma) &= (2 - \sigma)V_\tau'((2 - \sigma)t - \Theta)\tilde{\psi}_{\lambda-\epsilon} - V_\tau((2 - \sigma)t - \Theta)\left(d\tilde{\psi}''_{\lambda-\epsilon} + 2\tilde{\psi}'_{\lambda-\epsilon} + g(U_{KPP}(x - 2t))\tilde{\psi}_{\lambda-\epsilon}\right) \\ &+ \left(V_\tau((2 - \sigma)t - \Theta)\tilde{\psi}_{\lambda-\epsilon}\right)^3. \end{aligned}$$

Phase plane analysis of the traveling front equation for (4.1) gives V_τ' as a function of V_τ. In particular,

$$V_\tau' = \mu(\sigma)V_\tau(1 + r_-(V_\tau)) \quad \text{as } V_\tau \to 0, \tag{4.14}$$

for some function $r_-(V_\tau) < 0$ with $r_-(V_\tau) \to 0$ as $V_\tau \to 0$.

Returning to $N(z_\sigma)$, we recall that whenever $\tilde{\psi}_{\lambda-\epsilon} \neq 0$, then $\tilde{\psi}_{\lambda-\epsilon}$ solves (4.6). Using these two pieces of information, $N(z_\sigma)$ simplifies to,

$$\begin{aligned} N(z_\sigma) &= \left((2 - \sigma)\mu(\sigma) - \lambda + \epsilon\right) V_\tau((2 - \sigma)t - \Theta)\tilde{\psi}_{\lambda-\epsilon} + R_z(V_\tau, \tilde{\psi}_{\lambda-\epsilon}) \\ &= \left((2 - \sigma)\mu(\sigma) - (2 - s_v)\mu(s_v) + \epsilon\right) V_\tau((2 - \sigma)t - \Theta)\tilde{\psi}_{\lambda-\epsilon} + R_z(V_\tau, \tilde{\psi}_{\lambda-\epsilon}), \end{aligned} \tag{4.15}$$

where we have used (4.3) to substitute for λ in the second line. Here R_z is of quadratic order in V_τ and tends to zero as $\tau \to -\infty$. Since $\mu(\sigma) < \mu(s_v)$ we have that $(2 - \sigma)\mu(\sigma) - (2 - s_v)\mu(s_v) < 0$. Now, owing to (4.11) the linear coefficient of $V_\tau((2 - \sigma)t - \Theta)$ in (4.15) remains negative for all $\epsilon < \epsilon_0(\sigma)$. Consequently, for each σ and ϵ we can take $\tau_0(\sigma, \epsilon, \Theta)$ sufficiently negative so that $R_z(V_\tau, \psi_{\lambda-\epsilon})$ is smaller than the linear term and therefore we ensure $N(z_\sigma) < 0$ for $x - 2t > -\Theta$.

We have now shown that z_σ is a subsolution on the semi-infinite intervals on either side of $x - 2t = -\Theta$. It is easy to verify that z_σ is continuous at $x - 2t = -\Theta$ and that the derivatives on either side are negative. It remains to show that there exists a positive jump in the derivatives at this point, i.e.

$$\frac{\partial z_\sigma}{\partial x}(t, (2t-\Theta)^-) < \frac{\partial z_\sigma}{\partial x}(t, (2t-\Theta)^+) < 0,$$

so that the concatenation of these subsolutions is also a subsolution.

We first compute,

$$\frac{\partial z_\sigma}{\partial x}(t, (2t-\Theta)^-) = V_\tau'((2-\sigma)t - \Theta) = \mu(\sigma) V_\tau((2-\sigma)t-\Theta)\left(1 + r_-\left(V_\tau((2-\sigma)t-\Theta)\right)\right),$$

see (4.14). On the other hand, we compute,

$$\frac{\partial z_\sigma}{\partial x}(t, (2t-\Theta)^+) = V_\tau((2-\sigma)t-\Theta)\frac{d\tilde{\psi}_{\lambda-\epsilon}}{dx}(-\Theta) \tag{4.16}$$

Recall that as $\tau \to -\infty$, $V_\tau((2-\sigma)t - \Theta) \to 0$ and therefore so does $r_-(V_\tau)$. Given our choice of Θ, in particular (4.13), we find that our derivative condition holds in the limit as $\tau \to -\infty$. Further restricting $\tau_0(\sigma, \epsilon, \Theta)$ if necessary establishes $z_\sigma(t,x)$ as a subsolution for $(t,x) \in \mathbb{R}^+ \times \mathbb{R}$ for all $0 < \epsilon < \epsilon_0(\sigma)$ and $\tau < \tau_0(\sigma, \epsilon, \Theta)$.

■

These lemmas lead to a precise characterization of the selected wavespeed. Define the invasion point,

$$\delta(t) := \sup_{x\in\mathbb{R}}\left\{x \mid v(t,x) \geq \frac{\sqrt{g(1)}}{2}\right\}. \tag{4.17}$$

The selected spreading speed is then defined as,

$$s_{sel} := \lim_{t\to\infty}\frac{\delta(t)}{t}.$$

Theorem 3. *Assume that $g'(1) < 0$. Consider initial data, $0 \leq v_{init}(x) \leq \sqrt{g^*}$, a compact perturbation of the step function $\sqrt{g(1)}H(-x)$, with $H(x)$ the Heaviside step function. Suppose $\lambda \in (\lambda_{crit}, 0)$ is the principle eigenvalue of the operator H_g. Then, the asymptotically selected spreading speed for the v component of (4.4) is s_v, as given in (4.3).*

Proof: First, note that after some arbitrarily small amount of time, the initial condition will have been smoothed into a profile, $v_0(x)$, satisfying

- $0 < v_0(x) < \sqrt{g^*}$,
- $|v_0(x) - \sqrt{g(1)}| < Ce^{\alpha x}$ as $x \to -\infty$ for any $\alpha > 0$
- $|v_0(x)| < Ce^{-\alpha x}$ as $x \to \infty$ for any $\alpha > 0$.

By selecting an appropriate scalar multiple of ϕ_λ in Lemma 4.1 we can then find $w(t,x)$ from Lemma 4.1 so that $v_0(x) < w(0,x)$. Let $\delta_w(t) := \sup_{x\in\mathbb{R}}\{t \mid w(t,x) \geq \frac{\sqrt{g(1)}}{2}\}$. Then $s_{sel} < \liminf_{t\to\infty}\frac{\delta_w(t)}{t} = s_v$. Conversely, for any $2\sqrt{dg(1)} < \sigma < s_v$ and $0 < \epsilon < \epsilon_0(\sigma)$ there exists a $\tau < \tau_0(\sigma, \epsilon, \Theta)$ such that $z_\sigma(t,x) < v_0(x)$. In analogy to the previous case, we define $\delta_{z_\sigma}(t) := \sup_{x\in\mathbb{R}}\{t \mid z_\sigma(t,x) \geq \frac{\sqrt{g(1)}}{2}\}$. Then Lemma 4.2 implies that $s_{sel} \geq \sup_{2\sqrt{dg(1)}<\sigma<s_v}\limsup_{t\to\infty}\frac{\delta_{z_\sigma}(t)}{t} = s_v$. Therefore, $s_{sel} = s_v$.

■

We have now established that the accelerated speed, s_v, is the selected speed of propagation for the scalar equation

$$v_t = dv_{xx} + g(U_{KPP}(x-2t))v - v^3.$$

We now extend the result to initial data that consisting of compactly supported perturbations of Heaviside step functions in both the u and v component. We remark that in partially coupled systems of reaction-diffusion equations the selected spreading speed for the system is not always equal to that of the scalar reduction. We point the reader to [14] for such an example. Nonetheless, our analysis will show that such a reduction does not alter the selected wavespeed of (1.1). The following result of Bramson will be key.

Theorem 4. *[4] Let $0 \leq u_0(x) \leq 1$, where $u_0(x)$ is a compactly supported perturbation of a Heaviside step function. Then for all $\delta > 0$, there exists a $T(u_0, \delta)$ and a constant c_m such that*

$$\|u(t,x,u_0) - U_{KPP}(x - m(t))\|_{L^\infty} < \delta,$$

for all $t \geq T(u_0,\delta)$ for $m(t) = 2t - \frac{3}{2}\log(t) + c_m$.

Thus, after a sufficiently large period of time the u component will be pointwise close to a traveling front solution when considered in a moving frame with appropriate logarithmic correction to the speed. We will first show that, once the solution is sufficiently close to this traveling front solution then the sub and super solutions from Lemma 4.2 and Lemma 4.1 can be naturally adjusted to be sub and super solutions in the more general case.

Lemma 4.3. *Let u_0 be initial data for the u component of (1.1) satisfying $0 \leq u_0 \leq 1$, a compactly supported perturbation of the Heaviside step function $H(-x)$. Let $m(t)$ be given as in Theorem 4. Let ψ_λ be the unique, up to scalar multiplication, solution of (4.6) satisfying the asymptotic boundary condition (4.7). Then for any $\epsilon > 0$, there exists a $T(u_0,\epsilon) > 0$ so that*

$$w_\epsilon(t,x) = \min\left\{\sqrt{g^*}, e^{(\lambda+\epsilon)t}\psi_\lambda(x - m(t))\right\}, \tag{4.18}$$

is a super-solution for all $t > T(u_0)$ and all $x \in \mathbb{R}$.

Proof: That the constant $\sqrt{g^*}$ is a super solution follows as in Lemma 4.1. Now consider $\epsilon > 0$ and compute

$$\begin{aligned} e^{-(\lambda+\epsilon)t}N\left(e^{(\lambda+\epsilon)t}\psi_\lambda(x-m(t))\right) &= (\lambda+\epsilon)\psi_\lambda - m'(t)\psi'_\lambda - d\psi''_\lambda - g(u(t,x))\psi_\lambda + e^{2(\lambda+\epsilon)t}\psi_\lambda^3 \\ &= \left(\epsilon + g\left(U_{KPP}(x-m(t))\right) - g(u(t,x)) + \frac{3}{2t}\frac{\psi'_\lambda}{\psi_\lambda}\right)\psi_\lambda + e^{2(\lambda+\epsilon)t}\psi_\lambda^3. \end{aligned}$$

In light of Theorem 4, the difference between $g(U_{KPP}(x-m(t)))$ and $g(u(t,x))$ tends to zero as t gets large. Consider the quotient $\alpha = \frac{\psi'_\lambda}{\psi_\lambda}$. The evolution of α as a function of $\xi = x - m(t)$ is given by the Riccati equation

$$d\alpha' = -g\left(U_{KPP}(\xi)\right) + \lambda - 2\alpha - d\alpha^2,$$

from which it is easy to verify that the quantity $\frac{\psi'_\lambda}{\psi_\lambda}$ remains bounded. Thus, given any $\epsilon > 0$ there exists a $T(u_0,\epsilon)$ sufficiently large so that $N(w_\epsilon) > 0$ for all $x \in \mathbb{R}$ and $t > T$. This establishes (4.18) as a supersolution for all $\epsilon > 0$.

■

In the limit as $t \to \infty$, the supersolutions w_ϵ propagate to the right with asymptotic speed,

$$s_v + \frac{\epsilon}{d^{-1} - d^{-1}\sqrt{1 - dg(1) + d\lambda}}. \tag{4.19}$$

We now construct subsolutions.

Lemma 4.4. *Let u_0 be initial data for the u component of (1.1) satisfying $0 \le u_0 \le 1$, a compactly supported perturbation of the Heaviside step function $H(-x)$. Consider any σ satisfying $2\sqrt{dg(1)} < \sigma < s_v$. Let $m(t)$ be defined as in Theorem 4. Then, there exists $\epsilon_0(\sigma) > 0$, $T(u_0, \epsilon_0(\sigma)) > 0$, $\Theta(\sigma, \epsilon_0, T)$, $c_m(u_0) \in \mathbb{R}$ and $\tau_0(\sigma, \epsilon, \Theta, T)$ such that for all $0 < \epsilon < \epsilon_0(\sigma)$ and all $\tau < \tau_0(\sigma, \epsilon, \Theta, T) < 0$ we have that*

$$z_\sigma(t,x) = \begin{cases} V_\tau(x - m(t)) & \text{for} \quad x - m(t) < -\Theta \\ V_\tau(m(t) - \sigma t - \Theta)\tilde{\psi}_{\lambda-\epsilon}(x - m(t)) & \text{for} \quad x - m(t) \ge -\Theta, \end{cases} \tag{4.20}$$

is a subsolution for all $t > T$ and any $x \in \mathbb{R}$. Here, $\tilde{\psi}_{\lambda-\epsilon}(\cdot) := \max\{\psi_{\lambda-\epsilon}(\cdot), 0\}$, where $\psi_{\lambda-\epsilon}$ solves the ordinary differential equation in (4.6) with asymptotic boundary conditions as in (4.7) and with spectral parameter $\lambda - \epsilon$. We take $\tilde{\psi}_{\lambda-\epsilon}(-\Theta) = 1$.

Proof: We proceed as we did in the proof of Lemma 4.2 and consider $N(z_\sigma)$. Consider any $2\sqrt{dg(1)} < \sigma < s_v$. Select $\epsilon_0(\sigma)$ as was done in (4.9)-(4.11). As a result of Theorem 4, we can find $T(u_0, \epsilon_0) > 0$ and a constant c_m so that with $m(t) = 2t - \frac{3}{2}\log(t) + c_m$ we have

$$\frac{3}{2t} + (g(U_{KPP}(x - m(t))) - g(u(t,x))) < (2 - s_v)\mu(s_v) - (2 - \sigma)\mu(\sigma) - \epsilon_0(\sigma), \tag{4.21}$$

for all $t > T(u_0)$. We may now select Θ so that

$$g(u(t,x)) > g(1) \quad \text{for all} \quad x - m(t) < -\Theta \tag{4.22}$$

$$\mu(\sigma) < \frac{d\tilde{\psi}_{\lambda-\epsilon}}{d\xi}(-\Theta). \tag{4.23}$$

It remains to verify that by selecting τ_0 appropriately then (4.20) remains a subsolution for (1.1) for t sufficiently large. For $x - m(t) < -\Theta$, the same analysis applies using (4.22) as in Lemma 4.2 and z_σ is shown to be a subsolution there.

For $x - m(t) \ge -\Theta$ and on the interval where $z_\sigma \ne 0$ we have

$$\begin{aligned} N(z_\sigma) &= (m'(t) - \sigma)V_\tau'(m(t) - \sigma t - \Theta)\tilde{\psi}_{\lambda-\epsilon} \\ &\quad -V_\tau(m(t) - \sigma t - \Theta)\left(d\tilde{\psi}''_{\lambda-\epsilon} + m'(t)\tilde{\psi}'_{\lambda-\epsilon} + g(u(t,x))\tilde{\psi}_{\lambda-\epsilon}\right) + \left(V_\tau(m(t) - \sigma t - \Theta)\tilde{\psi}_{\lambda-\epsilon}\right)^3 \\ &= (2 - \frac{3}{2t} - \sigma)V_\tau'(m(t) - \sigma t - \Theta)\tilde{\psi}_{\lambda-\epsilon} \\ &\quad -V_\tau(m(t) - \sigma t - \Theta)\left(d\tilde{\psi}''_{\lambda-\epsilon} + 2\tilde{\psi}'_{\lambda-\epsilon} + g(U_{KPP}(x - m(t)))\tilde{\psi}_{\lambda-\epsilon}\right) + \frac{3}{2t}V_\tau(m(t) - \sigma t - \Theta)\tilde{\psi}'_{\lambda-\epsilon} \\ &\quad +V_\tau(m(t) - \sigma t - \Theta)\tilde{\psi}_{\lambda-\epsilon}\left(g(U_{KPP}(x - m(t)) - g(u(t,x))\right) + \left(V_\tau(m(t) - \sigma t - \Theta)\tilde{\psi}_{\lambda-\epsilon}\right)^3. \end{aligned}$$

Replacing $V_\tau'(m(t) - \sigma t - \Theta)$ with its expansion in V_τ as $\tau \to -\infty$ and using that $\tilde{\psi}_{\lambda-\epsilon}$ is a solution to a linearized eigenvalue problem (4.6), we can reduce this quantity to

$$\begin{aligned} N(z_\sigma) &= \left((2 - \sigma)\mu(\sigma) - \lambda + \frac{3}{2t} + (g(U_{KPP}(x - m(t))) - g(u(t,x))) + \epsilon\right)V_\tau\tilde{\psi}_{\lambda-\epsilon} \\ &\quad - \frac{3}{2t}\mu(\sigma)V_\tau'\tilde{\psi}_{\lambda-\epsilon} + R_z(V_\tau, \tilde{\psi}_{\lambda-\epsilon}). \end{aligned}$$

We replace $\lambda = (2 - s_v)\mu(s_v)$. Now, for any ϵ sufficiently small we observe that (4.21) implies that the terms multiplying $V_\tau\tilde{\psi}_{\lambda-\epsilon}$ are negative. The nonlinear remainder term can also be controlled by setting τ_0 smaller if necessary. Finally, since $\mu(\sigma) < 0$ and $V_\tau'(x - m(t) - \Theta) < 0$ we find that z_σ is a subsolution for $x - m(t) < -\Theta$.

■

Combining these two lemmas we have the following result.

Theorem 5. *Assume that $g'(1) < 0$. Consider initial data for system (1.1) satisfying $0 \leq u_0 \leq 1$ and $0 \leq v_0(x) \leq \sqrt{g^*}$, both compact perturbations of the Heaviside step functions $H(-x)$ and $\sqrt{g(1)}H(-x)$, respectively. Suppose $\lambda \in (\lambda_{crit}, 0)$ is the principle eigenvalue of the operator H_g. Then, the asymptotically selected spreading speed for the v component of (1.1) is s_v, as given in (4.3).*

Proof: Define the invasion point and selected speed as in (4.17). Fix u_0 and v_0 as above. For any finite time, the solutions $u(t,x)$ and $v(t,x)$ are exponentially localized in that they converge to their asymptotic limits at a rate greater than any exponential.

Let $\epsilon > 0$. Then Lemma 4.3 gives the existence of a $T(u_0, \epsilon) > 0$ so that w_ϵ in Lemma 4.3 is a super-solution for any positive scalar multiple of ψ_λ. Also, $0 < v(T(u_0,\epsilon),x) < \sqrt{g^*}$ and the solution converges to its asymptotic rest states faster than any exponential. Consequently, a scalar multiple of ψ_λ can be selected so that $v(t,x) < w_\epsilon(t,x)$ for all $t > T(u_0,\epsilon)$. This implies $s_{sel} \leq \liminf_{t\to\infty} \frac{\delta_{w_\epsilon}(t)}{t} = s_v + \frac{\epsilon}{\mu(s_v)}$.

Let $2\sqrt{dg(1)} < \sigma < s_v$. Lemma 4.4 implies that there exists an $\epsilon_0(\sigma) > 0$, such that for any $0 < \epsilon < \epsilon_0(\sigma)$ there exists $T(u_0, \epsilon_0(\sigma)) > 0$, $\Theta(\sigma, \epsilon_0, T) \in \mathbb{R}$ and $\tau_0(\sigma, \epsilon, \Theta, T) < 0$ such that $z_\sigma(t,x)$ defined in (4.20) is a subsolution for all $\tau < \tau_0$. These subsolutions converge exponentially to the asymptotic state $v = \sqrt{g(1)}$ as $x \to -\infty$ and terminate at some fixed value of $x - m(t)$. Since $0 < v(T,x) < \sqrt{g^*}$ we can find a $\tau < \tau_0$ so that $z_\sigma(t,x) < v(t,x)$ for all $t > T$ and $x \in \mathbb{R}$. This implies that $s_{sel} > \limsup_{t\to\infty} \frac{\delta_{z_\sigma}}{t} = \sigma$ for any $2\sqrt{dg(1)} < \sigma < s_v$.

Combining these two observations we find that the asymptotic speed of propagation for the v component of (1.1) is s_v.

■

Accelerated spreading induced by essential spectrum We have thusfar concentrated on the case where the principle eigenvalue of H_g exists. Of course, the rightmost point in the spectrum could also consist of essential spectrum. The techniques above generalize to this case and we will sketch the details.

First, we recall that the essential spectrum of H_g extends to the value

$$\lambda_{ess} = \max\{-d^{-1} + g(0), -d^{-1} + g(1)\}.$$

If $\lambda_{ess} > \lambda_{crit}$, then accelerated speeds are observed according to formula (4.3). Before proceeding we observe that $-d^{-1} + g(1) < \lambda_{crit}$. Thus, if accelerated spreading is to be induced by essential spectrum it must be due to the essential spectrum related to the state ahead of the Fisher-KPP front. This is summarized in the following result.

Lemma 4.5. *Assume that $\lambda_{ess} = -d^{-1} + g(0) < 0$ is the rightmost point in the spectrum of H_g. If $\lambda_{ess} > \lambda_{crit}$ then the selected spreading speed of the v component in (1.1) is*

$$s_v = 2 - \frac{d\lambda_{ess}}{-1 + \sqrt{1 - dg(1) + d\lambda_{ess}}}.$$

Since many of the calculations closely resemble those above, we will only sketch the proof here. Similar sub and super solutions can be found as were done in Lemma 4.3 and Lemma 4.4. Without a principle eigenfunction at hand several modifications are necessary. Instead, we will use exclusively solutions of the linearized eigenvalue problem (4.6) with asymptotic boundary condition (4.7). Let $\epsilon > 0$ and define

$$w_\epsilon = \{\sqrt{g^*}, e^{(\lambda_{ess}+\epsilon)t}\psi_{\lambda_{ess}}(x - m(t))\}.$$

This is a super-solution, which can be verified in a similar fashion to (4.3). It is important to note that $\psi_{\lambda_{ess}} > 0$.

Now consider any $2\sqrt{dg(1)} < \sigma < s_v$. Let

$$z_\sigma(t,x) = \begin{cases} V_\tau(x - m(t)) & \text{for} \quad x - m(t) < -\Theta \\ V_\tau(m(t) - \sigma t - \Theta)\tilde{\psi}_{\lambda-\epsilon}(x - m(t)) & \text{for} \quad x - m(t) \geq -\Theta, \end{cases} \tag{4.24}$$

where $\psi_{\lambda-\epsilon}$ is again a solution to (4.6) with appropriate asymptotic boundary condition. This function has oscillatory decay as $\xi \to \infty$. In contrast to Lemma 4.4, the cut-off function $\tilde{\psi}_{\lambda-\epsilon}$ is then chosen so that $\tilde{\psi}_{\lambda-\epsilon} \geq 0$ for all ξ. Proceeding as above, we can find conditions on ϵ, Θ, T and τ so that (4.24) is a subsolution.

Remark 4. *The speed associated to the state in the wake of the KPP front ($u = 1$) places a lower bound on the speed of propagation of the v component. On the other hand, the speed associated to the state ahead of the KPP front ($u = 0$) is not directly related to the selected speed. That is, parameter regimes exist where the accelerated speed is slower than the speed associated to the state ahead of the front.*

5 Numerical results

We compare our analytical predictions against numerical results. Spreading speeds are computed directly from (1.1) using a Crank-Nicholson finite difference scheme. Different choices of the inhomogeneity $g(u)$ yield similar results, so we consider only the quadratic nonlinearity,

$$g(u) = a + bu - bu^2.$$

The principle eigenvalues are also computed numerically using (2.3). Predicted versus observed spreading speeds show close agreement for a variety of parameter values, see Figure 3.

We also study the dynamics near the onset of locking and in particular the relationship between the principle eigenvalue of H_g and the distance between the two front interfaces. Corollary 1 establishes that this distance is proportional to the logarithm of the principle eigenvalue. The proportionality constant depends on the relationship between the eigenvalues $\nu_v^{\pm}$ with a change occurring as these eigenvalues pass through a $3:1$ resonance. Numerical corroboration of these results is more problematic. Recalling Lemma 3.6, let $\beta = \nu_v^-/\nu_v^+$ denote the ratio between these eigenvalues. When there exists a large gap between the eigenvalues $\nu_v^{\pm}$ (equivalent to $\beta > 3$ or $a < 3/4$), direct numerical simulations yield good agreement with the theory, see Figure 3. However, when the gap between these eigenvalues becomes more moderate, we find that data derived from direct numerical simulation does not produce data that obeys a convincing linear relationship between the length of front separation and the logarithm of the principle eigenvalue.

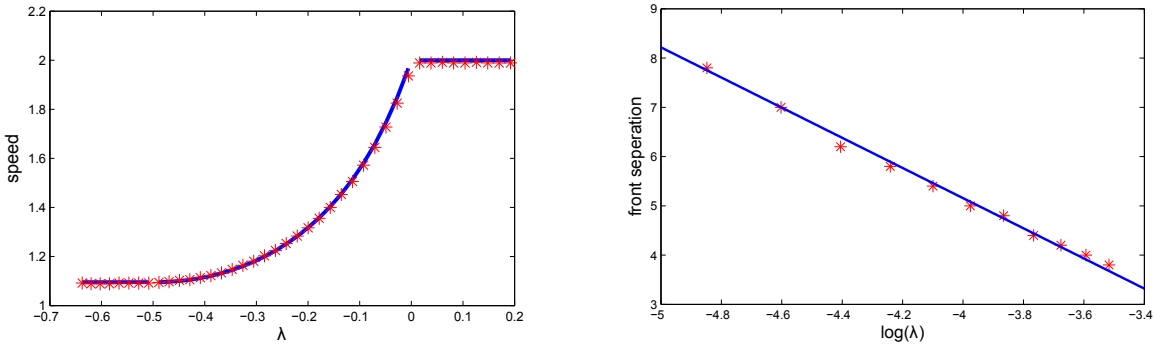

Figure 3: The figure on the left compares spreading speeds versus theoretical predictions for the model (1.1) with nonlinear inhomogenity $g(u) = a + bu - bu^2$ for a fixed value of $a = 0.3$ and $b \in [.4, 4.5]$. Instead of plotting speeds against the parameter b we plot speeds against the numerically computed value of the principle eigenvalue as the parameter b is varied. The $*$ are numerically computed spreading speeds and the solid lines are theoretical predictions based upon Theorem 1 and Theorem 2. On the right, we plot the logarithm of the principle eigenvalue versus the front separation in the locked case just above criticality ($b_{crit} \approx 3.63$). Again, the $*$ are numerically derived and the solid line has the slope predicted in Corollary 1.

To investigate this regime, we use the numerical continuation package AUTO, [10] and compute approximations for the actual front profiles found from the traveling wave equations (3.1). Numerical continuation can locate the approximate bifurcation point, b_{crit}, where the principle eigenvalue of H_g is zero. We can then plot front separation as a graph over $\log(b - b_{crit}) \sim \log(\lambda)$. Figure 4 illustrates this relationship. We found a reasonably good match between the slope computed from this data and the prediction in Corollary 1. As is expected, this linear relationship fails to hold for larger values of the bifurcation parameter. However, we also note that deviations exist for very small values of $b - b_{crit}$, or equivalently, for very large separation distances. A good linear fit is achieved for values of $\log(b - b_{crit}) \in [-10, -6]$ for values of $a < 3/4$. At

$a = 3/4$, the spatial eigenvalues $\nu_v^{\pm}$ pass through a $3:1$ resonance. Above this resonance value a similar linear relationship holds between the distance of front separation and the logarithm of the bifurcation parameter $b - b_{crit}$, although to find a good fit requires using more moderate values of the bifurcation parameter, namely $\log(b - b_{crit}) \in [-6, -3]$. A physical explanation for the deviation at very small values of $b - b_{crit}$ is elusive, but we suspect that this discrepancy can be explained by boundary effects that become non-negligible in the limit where the front separation tends to ∞.

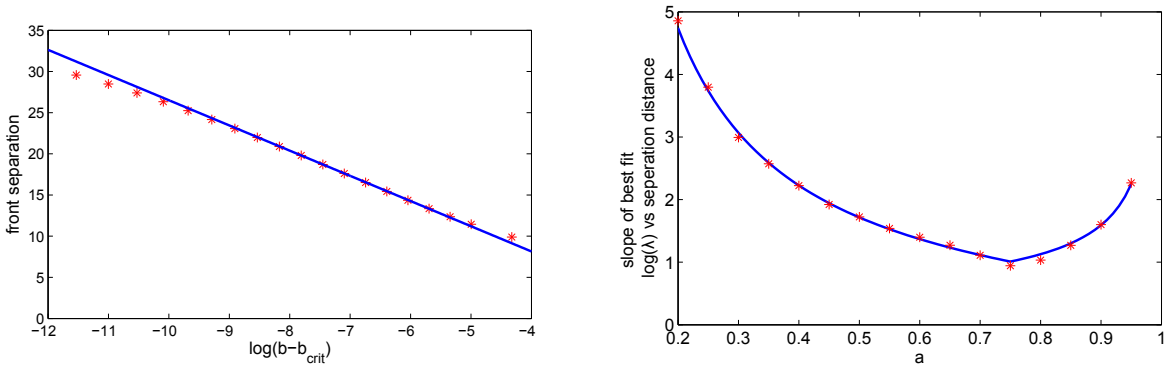

Figure 4: On the left, we fix $a = 0.3$ and graph $\log(b - b_{crit})$ against the length of front separation using numerically computed front profiles. Note that $b_{crit} \approx 3.63$ is the numerically calculated value of b for which the principle eigenvalue of H_g is zero. The solid line is the theoretical prediction from Corollary 1 while the $*$ are derived numerically using continuation. Note that there is an interval of considerable size for which the numerical and theoretical results match. On the right, the data denoted with asterisks is the slope of the best linear fit line for various values of a computed from the same numerically computed front profiles. The solid line plots the exact slope derived in Corollary 1. Note the cross over at $a = 3/4$ as the eigenvalues pass through resonance.

Acknowledgments

The research of MH was supported by the NSF (DMS-1004517). The research of AS was supported by the NSF (DMS-0806614).

A Example of a Subcritical Bifurcation

The bifurcation of the locked front that was established in Theorem 1 was found to be supercritical. That is, the principle eigenvalue is a bifurcation parameter and as this parameter passes through zero a bifurcation occurs leading to locked fronts. The bifurcation is supercritical since the locked fronts only occur when the principle eigenvalue is greater than the critical value of zero. As one can imagine, there are nonlinearities that give rise to subcritical bifurcations wherein nonlinear locked fronts exist for values of the bifurcation parameter that lie in the subcritical regime. Consider for example,

$$\begin{aligned} u_t &= u_{xx} + u(1-u) \\ v_t &= dv_{xx} + g(u)v + (1-g(u))v^2 - v^3. \end{aligned} \tag{A.1}$$

The v equation is again a rescaled version of Nagumo's equation, $v_t = dv_{xx} + v(v+a)(1-v)$, with $a = g(u)$. The selected wavespeed depends on the value of a and in contrast to the symmetric example considered in (1.1), there exists values of a for which the selected wavespeed is not the linear spreading speed. To be precise, when $a < 1/2$, the selected front is pushed and the speeds in these two regimes are,

$$s = \begin{cases} 2\sqrt{da} & \text{for} \quad a \geq \frac{1}{2} \\ \sqrt{2d}\left(\frac{1}{2} + a\right) & \text{for} \quad a < \frac{1}{2} \end{cases}.$$

Now take $g(u)$ as above with the modified stipulation that $g(u) < 1/2$. Then the pointwise v dynamics are always in the pushed Nagumo regime. By further imposing, $\sqrt{2d}(1/2 + g(1)) < 2$ and $\sqrt{2d}(1/2 + g(0)) < 2$, we find that the asymptotic spreading speeds ahead of and behind the KPP front remain slower than the KPP front itself.

A similar analysis to that of section 3 could be carried out for this example. We note that the sign of the Melnikov integral in (3.12) would now be positive due to the enhancement of the instability by the nonlinearity near the leading edge of the front. As a result, when varying the principle eigenvalue the tracked manifolds will intersect before their linearizations about the KPP front will. We show numerical evidence of this in Figure 5.

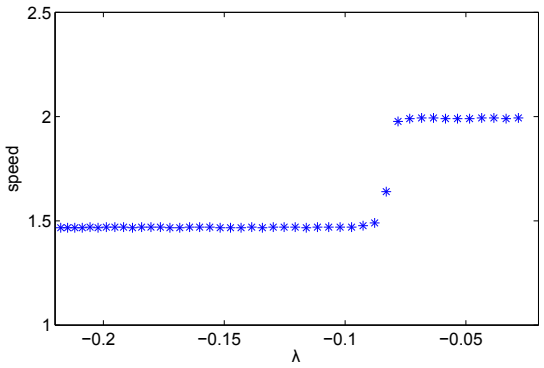

Figure 5: Selected spreading speeds of the v component for (A.1) plotted versus the principle eigenvalue. Notice the sudden transition to locking that occurs prior to the crossing through zero of the principle eigenvalue of H_g. This should be contrasted with the results in Figure 3 where the appearance of nonlinear locked fronts occurs only when the bifurcation parameter, i.e. the principle eigenvalue, is positive.

References

[1] J. Alexander, R. Gardner, and C. Jones. A topological invariant arising in the stability analysis of travelling waves. *J. Reine Angew. Math.*, 410:167–212, 1990.

[2] H. Berestycki, O. Diekmann, C. J. Nagelkerke, and P. A. Zegeling. Can a species keep pace with a shifting climate? *Bull. Math. Biol.*, 71(2):399–429, 2009.

[3] A. Bers. Space-time evolution of plasma instabilities-absolute and convective. In A. A. Galeev & R. N. Sudan, editor, *Basic Plasma Physics: Selected Chapters, Handbook of Plasma Physics, Volume 1*, pages 451–517, 1984.

[4] M. Bramson. Convergence of solutions of the Kolmogorov equation to travelling waves. *Mem. Amer. Math. Soc.*, 44(285):iv+190, 1983.

[5] E. Buzano and M. Golubitsky. Bifurcation on the hexagonal lattice and the planar benard problem. *Philosophical Transactions of the Royal Society of London. Series A, Mathematical and Physical Sciences*, 308(1505):pp. 617–667, 1983.

[6] J.-M. Chomaz, P. Huerre, and L. G. Redekopp. A frequency selection criterion in spatially developing flows. *Stud. Appl. Math.*, 84(2):119–144, 1991.

[7] E. A. Coddington and N. Levinson. *Theory of ordinary differential equations.* McGraw-Hill Book Company, Inc., New York-Toronto-London, 1955.

[8] G. Dee and J. S. Langer. Propagating pattern selection. *Phys. Rev. Lett.*, 50(6):383–386, Feb 1983.

[9] B. Deng. The Šil′nikov problem, exponential expansion, strong λ-lemma, C^1-linearization, and homoclinic bifurcation. *J. Differential Equations*, 79(2):189–231, 1989.

[10] E. J. Doedel, A. R. Champneys, T. F. Fairgrieve, Y. A. Kuznetsov, B. Sandstede, and X. Wang. Auto 97: Continuation and bifurcation software for ordinary differential equations (with homcont). Technical report, 2002.

[11] P. C. Fife and J. B. McLeod. The approach of solutions of nonlinear diffusion equations to travelling front solutions. *Arch. Ration. Mech. Anal.*, 65(4):335–361, 1977.

[12] R. A. Fisher. The wave of advance of advantageous genes. *Annals of Human Genetics*, 7(4):355–369, 1937.

[13] S. Heinze, G. Papanicolaou, and A. Stevens. Variational principles for propagation speeds in inhomogeneous media. *SIAM Journal on Applied Mathematics*, 62(1):pp. 129–148, 2001.

[14] M. Holzer. Anomalous spreading in a system of coupled Fisher-KPP equations. *preprint*, 2012.

[15] M. Holzer and A. Scheel. A slow pushed front in a Lotka Volterra competition model. *Nonlinearity*, 25(7):2151, 2012.

[16] A. J. Homburg and B. Sandstede. Chapter 8 - homoclinic and heteroclinic bifurcations in vector fields. In F. T. Henk Broer and B. Hasselblatt, editors, *Handbook of Dynamical Systems*, volume 3 of *Handbook of Dynamical Systems*, pages 379 – 524. Elsevier Science, 2010.

[17] A. Kolmogorov, I. Petrovskii, and N. Piscounov. Etude de l'equation de la diffusion avec croissance de la quantite' de matiere et son application a un probleme biologique. *Moscow Univ. Math. Bull.*, 1:1–25, 1937.

[18] J. Nolen, J.-M. Roquejoffre, L. Ryzhik, and A. Zlatoŝ. Existence and non-existence of fisher-kpp transition fronts. *Archive for Rational Mechanics and Analysis*, 203:217–246, 2012. 10.1007/s00205-011-0449-4.

[19] Y. Pomeau. Front motion, metastability and subcritical bifurcations in hydrodynamics. *Physica D: Nonlinear Phenomena*, 23(13):3 – 11, 1986.

[20] B. Sandstede and A. Scheel. Absolute and convective instabilities of waves on unbounded and large bounded domains. *Phys. D*, 145(3-4):233–277, 2000.

[21] L. Shilnikov. A contribution to the problem of the structure of an extended neighborhood of a rough equilibrium state of saddle-focus type. *Math. USSR Sbornik*, 10:91–102, 1970.

[22] W. van Saarloos. Front propagation into unstable states. *Physics Reports*, 386(2-6):29 – 222, 2003.

[23] H. F. Weinberger, M. A. Lewis, and B. Li. Anomalous spreading speeds of cooperative recursion systems. *J. Math. Biol.*, 55(2):207–222, 2007.

[24] J. Xin. Front propagation in heterogeneous media. *SIAM Rev.*, 42(2):161–230, 2000.